Institut National de la Recherche Scientifique
Centre Armand-Frappier Santé Biotechnologie

Metabolic labelling of the *Myxococcus xanthus* outer membrane

Par
Eric Ramirez Esquivel

Mémoire présenté pour l'obtention du grade de
Maître ès Sciences (M.Sc.)
en Microbiologie Appliquée

Jury d'évaluation

Président du jury et Examinateur interne	Prof. Annie Castonguay Centre Armand-Frappier Santé Biotechnologie Institut National de la Recherche Scientifique
Examinateur externe	Prof. Marylise Duperthuy Département de microbiologie, infectiologie et immunologie Université de Montreal
Directeur de recherche	Prof. Salim Timo Islam Centre Armand-Frappier Santé Biotechnologie Institut National de la Recherche Scientifique

ACKNOWLEDGMENTS

I would like to express my deepest gratefulness to my supervisor Pr. Salim Timo Islam for allowing me to pursue a M.Sc. degree in his laboratory, under his guidance and patience. I am confident that the project I took part in, presented a positive advance, that in the closest future will be starting to be listened in the science hallways.

I would like to continue by acknowledging my lab mates (Alec and Gokul) that shared with my several moments in the institute, which I will remind them for a good time in my life.
Fares Säidi, I will be always thankful for all the experiences, knowledge and guidance that I was able to go through with you.

Jose Luis Esquivel Reyes and Guadalupe Zamora, it is extremely hard to write your names and realize you are not here to share this moment with me. Thank you for always loving, inspiring and motivating me to be a better person in the society with all your wisdom and help. Yolanda and Silvia Esquivel, I am grateful for all you support and caring throught my life.

To my parents, Alma Rosa Esquivel Reyes and Rene Ramirez Castillo, I have only words of gratitude. An enormous reason that I was able to pursue a M.Sc. degree in a different country, without any monetary preoccupation, and always feeling in company and near my family. I want to share this achievement with both of you, after all the ups and downs in this period that with your guidance I was able to continue the pathway. Alma, thank you for being my supporter number one, no matter if I fail you have been always by my side. Rene, thank you for being the perspective and confidence that always helps me to focus and work hard each day to stay in my goal's pathway. ***Son y siempre serán mis ejemplos a seguir, mis guias y sobre todo los mejores padres que pudiera haber pedido. Infinitamente agradecido.***

Finally, I would like to extend my deepest gratitude to my life partner, Melany Nicole Juárez Velázquez. Words cannot express how important your time, attention and company helped me achieving this success. Thank you for always being by my side guiding me, supporting me, questioning me and loving me. I firmly believe that this success can help us to have the beginning we seek for our family, as well as the first of many other achievements both personally and as a couple. ***I will always love you, my beautiful and successful life partner.***

RÉSUMÉ

Le remodelage de la surface des cellules bactériennes est un phénomène omniprésent pour maintenir les connexions avec le substrat et / ou d'autres cellules, facilitant ainsi la communication, la coordination comportementale et la résidence à long terme. Chez les bactéries à Gram négatif, la surface cellulaire est composée en grande partie de lipopolysaccharide (LPS) dans le feuillet externe de la membrane externe (ME). Avec la bactérie modèle Gram négatif *Myxococcus xanthus* (membre des δ-proteobactéries), les agrégats cellulaires sont connectés les uns aux autres via des réseaux de tubes dérivés de la ME (TME) et des chaînes de vésicules (VME) composées de LPS. Les VME sont omniprésentes chez les bactéries à Gram négatif et sont impliquées dans la communication, le transfert d'ADN, la digestion des nutriments et la dissémination des toxines ; cependant, le mécanisme d'extrusion de la ME est mal compris généralement. Pour étudier ce phénomène en temps réel, on a besoin d'une méthode pour marquer le LPS sans tuer les bactéries. Mes études m'ont permis de développer un marquage de la ME de M. xanthus, par fluroescence via l'incorporation métabolique de Kdo-N_3 synthétisé, suivi de l'attachement covalent au groupe -N_3 avec DBCO-sulforhodamine via une réaction de chimie « clic ». Cela a permis le premier marquage spécifique du LPS dans la ME de *M. xanthus*. Des tests de physiologie de *M. xanthus* en ce qui concerne la motilité unicellulaire et de groupe, ainsi que la formation des corps fructifères ont été réalisés. Aucune différence à l'échelle de la communauté n'a été observée au cours des différentes étapes du cycle de vie de *M. xanthus* suite aux marquage par clic (Kdo-N_3 et DBCO-sulforhodamine). De plus, une vérification de marquage via une réaction clic de la ME a été réalisée par une extraction de LPS, par la méthode de Hitchcock et Brown ; cet échantillon de LPS marqué a été séparé par électrophorèse sur un gel SDS, suivi d'une analyse utilisant un scanner Typhoon, révélant un modèle d'échelle fluorescente en gel compatible avec l'incorporation réussie du Kdo-N_3 et le marquage chimique par clic du sucre synthétique dans la ME de *M. xanthus*.

Mots-clés : **membrane externe, chimie « clic », Kdo, lipopolysaccharide (LPS)**

ABSTRACT

Remodelling of the bacterial cell surface is a ubiquitous phenomenon for maintaining connections with the substratum and/or other cells, thus facilitating communication, behavioral coordination, and long-term residence. In Gram-negative bacteria, the cell surface is composed largely of lipopolysaccharide (LPS) in the outer leaflet of the outer membrane (OM). With the model Gram-negative δ-proteobacterium *Myxococcus xanthus*, cell aggregates become connected to each other over distances via networks of OM tube (OMTs) and vesicle (OMV) chain structures composed of LPS. OMVs are ubiquitous in Gram-negative bacteria and implicated in communication, DNA transfer, nutrient digestion, and toxin delivery; however, the mechanism of OM extrusion is poorly understood. To study this phenomenon in real time, a method to label the LPS is required, one which does not impact cell viability. During my studies, I successfully fluorescently labelled the *M. xanthus* OM via the metabolic incorporation of in-house-synthesized Kdo-N_3, followed by "click" chemistry-based covalent attachment of DBCO-sulforhodamine to the -N_3 moiety. This allowed for the first-ever LPS-specific labelling of the *M. xanthus* OM. Testing of *M. xanthus* physiology with respect to single-cell and group motility, as well as fruiting body formation were carried out. No differences regarding community-wide effects were observed during the various stages of the *M. xanthus* life cycle with the corresponding permutations of click-labelling components (Kdo-N_3 and DBCO-sulforhodamine). Moreover, OM labelling was successfully verified via extraction of LPS, labelled via a "click" reaction, by the Hitchcock & Brown method; this LPS was resolved on a gel via SDS-PAGE gel, followed by analysis with a Typhoon scanner, revealing an in-gel fluorescence ladder pattern consistent with successful Kdo-N_3 incorporation and click chemistry labelling of the synthetic sugar in the *M. xanthus* OM.

Keywords: **outer membrane, click chemistry, Kdo, lipopolysaccharide (LPS)**

SOMMAIRE RÉCAPITULATIF

Since this thesis is written in English, this section presents a French résumé, as required by the program. The figures cited in this section can be found in the main document.

Marquage métabolique de la membrane externe de *Myxococcus xanthus*

INTRODUCTION

L'ENVELOPPE DES CELLULES BACTERIENNES

Structure de l'enveloppe bactérienne

L'enveloppe des cellules bactériennes est structurée en l'un des deux types d'arrangements, appelés Gram positif ou Gram négatif, en fonction de la capacité des cellules à retenir le colorant cristal violet (« positif ») au lieu du contre-colorant safranine (« négatif »). Les cellules Gram positives contiennent deux couches : la membrane interne (MI) et la couche de peptidoglycane (PG). La première est une bicouche phospholipidique qui englobe le contenu cytoplasmique de la cellule. La paroi cellulaire du PG se trouve à l'extérieur de la MI et constitue un maillage d'unités répétées d'acide disaccharide N-acétylglucosamine–N-acétylmuramique, qui sont réticulées par des chaînes latérales pentapeptidiques. Chez les bactéries à Gram positif, la paroi cellulaire contient plusieurs couches de PG. En raison de sa rigidité, le sacculus de PG détermine la forme des cellules **(Fig. 1)**.

Chez les bactéries à Gram négatif, l'enveloppe cellulaire est composée de trois structures principales, dont une MI, une membrane externe ME, et une mince couche de PG dans l'espace périplasmique entre la MI et la ME. La ME est une bicouche asymétrique contenant en grande partie des phospholipides dans le feuillet périplasmique et le glycolipide lipopolysaccharide (LPS) dans le feuillet externe. La ME est donc le principal compartiment de distinction entre les bactéries à Gram négatif et à Gram positif. Toutes les composantes de l'enveloppe cellulaire Gram négative sont ainsi synthétisées dans le cytoplasme ou à la surface de la MI. Ces composantes doivent être transportées du cytoplasme ou retournées à travers la MI.

Le rôle du LPS

La couche de LPS est essentielle à l'intégrité de l'enveloppe cellulaire et joue un rôle critique dans la fonction de barrière de la ME. La partie membranaire du LPS, connue sous le

nom de lipide A **(Fig. 2)**, est un disaccharide de glucosamine avec généralement six ou sept chaînes acyles. L'oligosaccharide de noyau est joint à la partie lipide A ; cela peut servir de région de liaison au motif distal de l'antigène O (OAg) d'une molécule de LPS. L'OAg est la partie d'une molécule de LPS qui est responsable de la spécificité sérotypique de diverses souches bactériennes. Les groupes phosphates liés au lipide A sur les molécules LPS adjacentes dans la ME sont généralement pontés par des cations divalents comme le Mg^{2+}, servant à neutraliser la charge négative des groupes de phosphate. Les chaînes acyles du lipide A sont largement saturées, ce qui facilite un agencement serré, confèrant une faible fluidité et perméabilité à la ME. L'environnement non fluide formé par les molécules LPS est une barrière très efficace contre les molécules hydrophobes, de plus, elle permet la diffusion de molécules hydrophiles de plus de 700 Daltons. Ce qui fait que la ME est une barrière très efficace, sélective et perméable.

PHYSIOLOGIE DES MYXOBACTERIES

Les myxobactéries sont caractérisées par un mode de vie social. Ces interactions sociales jouent un rôle décisif dans sa croissance, sa motilité et son développement, et permettent aux cellules myxobactériennes de s'organiser en modèles spatiaux distincts et de se nourrir en coopération. *Myxococcus xanthus* est devenu le système modèle prééminent pour comprendre la génétique et les mécanismes moléculaires impliqués dans le comportement social des myxobactéries et plus largement les origines de la multicellularité chez les organismes supérieurs.

Myxococcus xanthus

Myxococcus xanthus appartient à la classe « delta » des protéobactéries. Les myxobactéries sont présentes partout dans l''environnement et ont la capacité de prédation lorsqu'elles sont en présence de micro-organismes proies. Le mode de vie social de *M. xanthus* dépend essentiellement de la capacité des cellules à afficher un mouvement actif. Si elles sont présentes sur une surface solide et à une densité cellulaire élevée, les cellules de *M. xanthus* s'auto-organisent en trois modèles spatiaux morphologiquement distincts : des colonies en expansion, des ondulations, ou des fructifications. Le modèle formé dépend en grande partie de l'état nutritionnel des cellules. En présence de nutriments, les cellules motiles en forme de bâtonnet se développent, se divisent et forment des colonies en expansion. Les cellules situées au bord d'une colonie se répartissent de manière coordonnée sur la surface, formant une structure mince en forme de *flare*. En absence de nutriments, le comportement de propagation

est limité et les cellules initient un programme de développement qui aboutit à la formation de corps fructifères multicellulaires remplis de myxospores **(Fig. 5)**.

Systèmes de motilité de *M. xanthus*

M. xanthus se déplace sur des surfaces en utilisant deux formes de motilité. La première est la motilité de type *gliding*, impliquant des cellules individuelles, utilisant le transport dirigé à travers de la cellule d'un complexe protéique trans-enveloppe. Quand ce complexe se fixe au substrat à l'extérieur de la cellule, celui-ci continue d'être transporté, mais ne se déplace plus. La cellule avance par rapport au complexe immobilisé sur le substrat. La deuxième forme de motilité est celle médiée par l'extrusion et la rétractation des pilis de Type IV (PT4), impliquant des groupes de cellules.

Dynamisme de le ME de *M. xanthus*

La ME *de M. xanthus* présente des propriétés dynamiques qui ont un impact sur la physiologie complexe de la bactérie. Dans les biofilms multicellulaires, les cellules de *M. xanthus* se sont révélées connectées via des réseaux de chaînes de vésicules de la ME (VME) et des projections de tubes de la ME (TME). Lorsque les cellules de *M. xanthus* sont en contact les unes avec les autres, les cellules compatibles peuvent fusionner leur MEs et échanger des lipides et des protéines ; quand ces cellules se séparent, si elles n'ont pas encore fendu la synapse entre les ME fusionnées, un TME peut se former. Compte tenu de la nature dynamique de la ME de *M. xanthus*, des connaissances mécanistiques plus approfondies sur les divers processus décrits ci-dessus sont nécessaires. De plus des méthodes permettant de visualiser et d'analyser spécifiquement ce compartiement cellulaire, doivent être développées.

Marquage de la ME

Une méthode populaire de marquer la ME, pour faire de l'imagerie de bactéries vivantes, consiste à génétiquement encoder des protéines fluorescentes de ce compartiment cellulaire. D'habitude, des fluorochromes comme sfGFP (*superfolder GFP*) ou mCherry sont fusionnés avec une protéine impliquée dans le tri, ce qui amène le fluorochrome vers le feuillet périplasmique de la ME. Dans ce cas, la périphérie de la cellule est marquée avec de la fluorescence, mais ce n'est pas le feuillet de la ME à la surface qui émet le signal fluorescent. Comme ces fluorochromes peuvent être encodés dans un chromosome ou un plasmide, il est possible d'induire une expression constitutive ou inductible, selon les besoins.

Par contre, des colorants fluorescents peuvent être utilisés d'une façon non-spécifique en s'intercalant entre les lipides de la ME. Ces molécules peuvent se diffuser partout dans les membranes pour donner lieu à un marquage périphérique homogène. Mais cette méthode ne permet pas de marquer spécifiquement les molécules de LPS.

LA CHIMIE « CLIC »

La chimie « clic » peut être définie comme une série de réactions (i) à haut rendement, (ii) de large portée, (iii) utilisant des réactifs qui peuvent être éliminés sans chromatographie, (iv) stéréospécifiques, (v) simples à réaliser, et (vi) peuvent avoir lieu en milieu aqueux. Plusieurs types de réactions, remplissant ces critères, ont été identifiés.

Types de réactions de la chimie « clic »

Les réactions de la chimie « clic » sont classées en deux groupes distincts : catalysées par le cuivre (Cu) ou non. La réaction de la cycloaddition « clic » azoture-alcyne catalysée par le Cu(I) (CuAAC) repose sur la présence d'ions Cu(I), tandis que la réaction « clic » azoture-alcyne (SPAAC) et la ligature tétrazine-alcène se déroulent efficacement en l'absence de catalyseur. La réaction azoture-alcyne sans cuivre est entravée par l'instabilité des alcynes et par la lente cinétique. Par conséquent, les réactions favorisées par la souche avec les cyclooctynes et la ligature tétrazine-alcène, respectivement, suscitent donc plus d'intérêt.

1. Réaction de chimie « clic » azoture-alcyne catalysée par Cu (I) (CuAAC):

Puisque les alcynes terminaux sont assez peu réactifs en présence d'azoture, l'efficacité d'une réaction CuAAC dépend fortement de la présence d'un catalyseur métallique tel que le cuivre (Pathak *et al.*) à l'état d'oxydation + 1 (Cu(I)). Différentes sources de cuivre et réactifs de réduction sont disponibles. Cependant, l'utilisation du sulfate de cuivre ($CuSO_4$) en tant que source de cuivre en combinaison avec l'ascorbate comme agent réducteur est recommandée pour la plupart des applications de marquage de biomolécules. L'utilisation des réactions CuAAC dans les cellules vivantes est entravée par la toxicité des ions Cu(I) **(Fig. 8)**.

2. Réaction de chimie « clic » l'azoture-alcyne (SPAAC) :

Une méthode de marquage des azotures sans cuivre, et donc non toxique, est la réaction de chimie « clic » azoture-alcyne (SPAAC). Les réactions SPAAC reposent sur l'utilisation de cyclooctynes contraintes qui possèdent une énergie d'activation remarquablement diminuée par rapport aux alcynes terminaux et ne nécessitent donc pas de

catalyseur exogène. Un certain nombre de dérivés de cyclooctyne structurellement variés (par exemple DIFO, BCN, DIBAC, DIBO, ADIBO) et différant fortement en termes de cinétique de réaction ont été développés **(Fig. 9)**.

3. Ligation tétrazine-alcène :

La ligation tétrazine-alcène constitue une méthode de marquage de biomolécules non-toxique, d'une vitesse inégalée, qui convient parfaitement au marquage cellulaire *in vivo* et aux applications à faible concentration. Une molécule A fonctionnalisée par la tétrazine réagit avec une molécule B fonctionnalisée par un alcène terminal ou contraint, formant ainsi un conjugué stable A-B via un fragment dihydropyrazine. Un certain nombre de dérivés d'alcène et de tétrazine structurellement variés, différant fortement en termes de cinétique de réaction et de stabilité, ont été développés. Le TCO a été sélectionné étant donné sa plus grande réactivité vis-à-vis de la tétrazine **(Fig. 10)**.

Marquage métabolique utilisant le sucre synthétique Kdo-N_3 et la chimie « clic »

Kdo-N_3 représente une version modifiée de l'acide 3-désoxy-D-manno-oct-2-ulosonique (Kdo), un sucre retrouvé dans la paroi cellulaire chez les plantes et dans l'oligosaccharide de noyau, partie essentiellelle pour le LPS chez les bactéries à Gram négatif. La modification -N_3 se trouve sur le 8e carbone de la molécule.

En tant que nouvelle technologie, en poussant la plante *Arabidopsis thaliana* en présence de Kdo-N_3, le sucre synthétique a pu être marqué avec un fluorochrome dans le rhamnogalacturonan-II de la paroi cellulaire via une réaction CuAAC. De plus, en incubant diverses souches bactériennes à Gram négatif en présence de Kdo-N_3, il fut possible de marquer la périphérie des cellules avec des fluorochromes via des réactions CuAAC ou SPAAC ; ce marquage est possible grâce à l'omniprésence de Kdo dans l'oligosaccharide de noyau du LPS à la surface des cellules.

PERTINENCE

Le remodelage de la surface des cellules bactériennes est un phénomène omniprésent pour maintenir les connexions avec le substrat et/ou d'autres cellules, facilitant ainsi la communication, la coordination comportementale et la résidence à long terme. Compte tenu de son mode de vie social complexe, la δ-proteobactérie à Gram négatif *Myxococcus xanthus* est devenue le modèle pour étudier les interactions ME-dépendantes chez les bactéries. Lors des carences nutritives, les cellules individuelles s'assemblent en agrégat qui maturent pour former des corps fructifères contenant de myxospores. Dans les agrégats de *M. xanthus*, les cellules se connectent les unes aux autres via des réseaux de TMEs et des chaînes de VMEs composées de LPS. Les VMEs sont omniprésentes dans les bactéries à Gram négatif et impliquées dans la communication, la digestion des nutriments et la délivrance de toxines ; cependant, le mécanisme de l'extrusion de la ME en général est mal compris. Pour étudier ce mécanisme en temps réel avec la bactérie modèle *M. xanthus*, un système de marquage par fluorescence de LPS n'affectant pas la viabilité des cellules est requis.

J'émets l'hypothèse que la ME de* M. xanthus *peut être marquée métaboliquement via l'importation de Kdo-N_3 dans la cellule, suivi par l'incorporation de ce sucre synthétique dans les molécules de LPS naissant ; ces molécules sont d'abord transportées vers la ME et intégrées à la surface des cellules. J'émets également l'hypothèse que ces cellules ne sont pas compromises pour l'obtention de résultats physiologiques normaux.

Pour tester ces hypothèses, j'ai d'abord synthétisé le Kdo-N_3 *in vitro* (en collaboration avec le laboratoire du Pr Charles Gauthier). L'importation et l'incorporation de Kdo-N_3 dans la ME de *M. xanthus* ont ensuite été testées via la supplémentation de cultures liquides avec Kdo-N_3, suivi d'un marquage par fluorescence basé sur la chimie « clic » des groupes -N_3 exposés à la surface cellulaire. Ce marquage de LPS a été vérifié via l'analyse de la périphérie des cellules intactes par microscopie à fluorescence, et par extraction de LPS « cliqué » suivi par la détection des bandes de LPS fluorescentes après électrophorèse. L'effet de l'incorporation de Kdo-N_3 sur la physiologie bactérienne a été étudié via les tests de motilité de type *gliding*, motilité médiée par les PT4s, et formation des corps fructifères. Aucun de ces tests n'a indiqué de différence par rapport aux cellules non traitées, ce qui suggère que l'incorporation de Kdo-N_3 dans le LPS de *M. xanthus* est physiologiquement inoffensive.

METHODES ET RESULTATS

SYNTHESE CHIMIQUE DE KDO-N_3

Compte tenu du succès de la fonctionnalisation de la ME avec Kdo-N_3 chez d'autres espèces bactériennes, et pour poursuivre nos expériences, nous avons d'abord optimisé la synthèse de notre propre Kdo-N_3, car il est commercialement coûteux (1500 $ pour 10 mg).

La synthèse a commencé avec l'introduction d'un groupement trityle sélectif primaire (triméthylphényle). De ce fait, la formation du cycle furanose a été activée, accédant ainsi au groupement hydroxyle primaire C-5. Le produit trityle brut a été directement traité avec Ac_2O et de la pyridine afin d'acétyler les autres groupements hydroxyles. Une réaction de déprotection sélective du trityle, soigneusement contrôlée, a été effectuée sur le composé en le chauffant dans une solution aqueuse à 80% aq. AcOH. Le produit alcoolique primaire obtenu a été tosylé dans des conditions standard de TsCl dans la pyridine. Le produit tosylé a ensuite été chauffé avec du NaN_3 à une température de 80 °C pour finalement insérer le fragment azoture. La déprotection Zemplén des groupes acétate des composés a finalement mené à la formation de 5-D-N_3-arabinopyranose.

Contrairement à la procédure de Cornforth standard (qui implique un excès d'arabinose et d'acide oxaloacétique), un excès d'acide oxaloacétique a été utilisé. À cet égard, la procédure de Cornforth modifiée a été effectuée en traitant le matériau de départ avec 2,5 équivalents d'acide oxaloacétique dans H_2O. L'environnement du solvant a été maintenu à pH 11 en utilisant une solution aqueuse de NaOH. Elle a été suivie par une étape de décarboxylation catalysée par $NiCl_2$•$6H_2O$ sous pH acide maintenu par AcOH concentré. Le mélange brut a été passé à travers une colonne de résine échangeuse d'anions, élué avec une solution à gradient linéaire de NH_4HCO_3 aqueux **(Fig. 20)**.

Le composé Kdo-azoture (Kdo-N_3) souhaité a été obtenu avec un rendement de 65%, équivalent à une valeur commerciale de 150 000$.

MARQUAGE DE LA MEMBRANE EXTERNE PAR LA CHIMIE « CLIC »

Pour tester le marquage par la chimie clic de la ME de *M. xanthus*, un protocole a été mis en place car l'utilisation de Kdo-N_3 n'a jamais été rapportée pour cette bactérie. Donc, la bactérie a été mise en culture liquide, de petit volume, en présence ou en absence de Kdo-N_3. Après avoir rincé le culot avec le tampon PBS, les cellules ont été traitées avec DBCO-sulforhodamine dans le but de générer une liaison covalente entre des groupes -N_3 du LPS

modifié exposé sur la surface des bactéries et le motif DBCO lié au fluorochrome sulforhodamine (via une réaction SPAAC) **(Fig. 21)**.

Microscopie à fluorescence des cellules individuelles

En analysant les cellules « cliquées » sur des géloses d'agar via la microscopie à fluorescence, il a été possible de visualiser la fluorescence rouge des cellules, ce qui correspond au signal de sulforhodamine. Ces données suggèrent que (i) le Kdo-N_3 est bien importé par les cellules, (ii) le sucre synthétique est bien incorporé dans les nouvelles molécules de LPS synthétisé à la MI, (iii) ce LPS modifié est transporté à travers le périplasme vers la ME, et (iv) le LPS modifié est bien inséré dans le feuillet externe de la ME **(Fig. 22)**.

Analyses phénotypiques de *M. xanthus*

L'effet d'avoir integré le LPS modifié avec Kdo-N_3 sur la physiologie de *M. xanthus* a ensuite été testé. Pour ce faire, les cellules ont été introduites sur géloses contenant du milieu riche (avec différentes concentrations d'agar pour rendre les matrices dures ou molles) ou du milieu pauvre, puis incubé à 32 ºC. Après 24 h, sur les géloses « riches et dures », la présence des flares a pu être observée au pourtour de l'essaim, ce qui permet d'observer la motilité de type *gliding*. Après 48 h, sur les géloses « riches et molles », l'expansion des essaims fut observée, indiquant la motilité sociale médiée par la fonction des T4Ps. Après 72 h, sur les géloses « pauvres », la formation des corps fructifères fut étudiée, indiquant un cycle de développement standard. En comparaison avec des cellules de référence qui n'ont pas reçu le sucre synthétique, les cellules produisant du LPS modifié avec Kdo-N_3 ne montraient pas de différences en flares au bord de l'essaim, ni dans l'expansion de l'essaim médié par les PT4s, ni dans la formation des corps fructifères. Tout bien consideré, l'intégration de Kdo-N_3 dans le LPS de *M. xanthus* n'impacte pas la physiologie globale de la bactérie **(Fig. 23)**.

Extraction du LPS de *Myxococcus xanthus*

Pour soutenir la proposition que Kdo-N_3 soit bien intégré dans la structure du LPS, le LPS des cellules « cliquées » avec DBCO-sulforhodamine a été isolé en utilisant le protocole développé par Hitchcock et Brown. Pour ce faire, les cellules culottées ont été suspendues en tampon « Hitchcock et Brown » (un tampon de lyse contenant du SDS), puis bouillies pour permettre la lyse des cellules. Puis, les lysats ont été traités avec Protéinase K pendant une nuit pour digérer toutes les protéines. L'échantillon sans protéines obtenu a été migré sur un gel de polyacrylamide pour séparer les différentes bandes correspondant au LPS. Ce gel a été

visualisé en utilisant un appareil Typhoon afin de détecter les signaux fluorescents. Comme prévu, une zone fluorescente de poids moléculaire élevé a été détectée dans le gel, ce qui est cohérent avec la taille des molécules du LPS contenant des lipides A, de l'oligosaccharide de noyau (contenant un sucre Kdo-N_3 « cliqué ») et des longueurs variables d'antigène O.

Par conséquent le Kdo-N_3 semble pouvoir s'intégrer légitimement dans le LPS de *M. xanthus* **(Fig. 24)**.

DISCUSSION ET PERSPECTIVES

L'IMPORTANCE DE LA SYNTHESE CHIMIQUE DU KDO-N_3

Pour ce projet, la synthèse de Kdo-N_3 a été effectuée afin de réaliser les expériences expliquées dans ce document. La synthèse de cette molécule peut être considérée comme efficace en termes de temps et d'argent. La synthèse a été effectuée sur une période d'environ 2 mois. L'efficacité des procédures était variable, puisque cette synthèse avait un protocole strict à suivre. En suivant des procédures normalisées dans la littérature, nous avons rencontré des difficultés. Ceci nous a conduit à déterminer et développer une voie de synthèse plus optimale. Au delà du temps de synthèse de Kdo-N_3, le prix commercial de ce produit peut être un problème. En effet cette synthèse est complexe, et nécessite un investissement considerable en temps et en argent, conditions qui causent sont élevé prix commercial.

La méthodologie de chimie Kdo-N_3 et « clic » sont en cours de modification afin de résoudre les besoins réels du domaine, offrant une approche attrayante pour la détection des bactéries à Gram négatif. Le sucre peut être importé par les cellules et incorporé à la place de Kdo natif dans les molécules de LPS naissant. Le LPS fonctionnalisé par azoture qui en résulte peut ensuite être détecté via la chimie « clic » catalysée par le Cu (I) ou sans Cu (I).

La valeur commerciale de Kdo-N_3 (415,11 EUR pour 2,5 mg) étant un facteur limitant pour le développement de nouveaux projets, il est important d'élaborer une méthode efficace pour le synthétiser.

L'IMPORTANCE DE LA TECHNOLOGIE KDO-N_3 ET LA CHIMIE « CLIC »

Lors de la sélection de la méthodologie pour le marquage de la ME de *M. xanthus*, il fallait prendre en compte les effets possibles des marqueurs sur le comportement ainsi que les possibles modifications cellulaires chez la bactérie. L'une des principales raisons de la sélection de la chimie « clic » était que cette réaction ne nécessite pas de catalyseur comme le cuivre qui est hautement toxique pour les cellules, et est capable d'affecter les caractéristiques sociales et physiologiques de *M. xanthus*

La technologie utilisée (la chimie « clic ») et les protocoles développés pour le marquage cellulaire *in vivo* de ce projet ont construit une base solide pour le développement de nouveaux projets. Toutefois, avant de discuter de l'avenir de ce projet, un renforcement de données expérimentales supplémentaires est nécessaire pour augmenter la robustesse des données et confirmer les conclusions qui ont été présentées. L'expérimentation supplémentaire du marquage de fluorescence unicellulaire avec la méthodologie de chimie « clic » et l'analyse

sociale et physiologique de *M. xanthus* sont les prochaines expériences à suivre afin d'avoir une compréhension complète du comportement des interactions unicellulaires et sociales que *M. xanthus* peut présenter.

Il y a deux continuités possibles avec cette technique incroyable. Le premier projet sera d'examiner la production « active » vs « passive » de TME au fil du temps. La méthodologie de marquage cellulaire peut être utilisée afin de démontrer que les TMEs ne sont pas simplement une excroissance du raccourcissement cellulaire pendant la sénescence. Les TMEs générés par des cellules fluorescentes « cliquées » pourraient être imagés au fil du temps par microscopie à fluorescence et les données obtenues peuvent être analysées dans un logiciel d'imagerie tel qu'ImageJ qui dispose de tous les outils nécessaires à l'analyse du comportement d'une cellule.

Le deuxième objectif qui pourrait être poursuivi avec la méthodologie de la chimie clic est l'identification et la caractérisation des protéines responsables de l'extrusion de la ME. Comme les TMEs sont générés aux pôles, toutes les machines associées doivent être localisées de la même manière ; ainsi, après induction de la production de VME polaire (et centrifugation différentielle pour les isoler) dans les cellules élaborant Kdo-N_3, ces cellules peuvent être lysées par une méthode mécanique. Bénéficiant à nouveau de la chimie « clic », le matériau total de la ME peut être isolé sélectivement via la liaison covalente du LPS aux billes magnétiques liées au DBCO, suivi par le retrait des billes magnétiques du mélange. Ceci empêcherait donc la contamination par des vésicules et des protéines dérivées de la MI.

Les échantillons de la ME isolés magnétiquement peuvent être portés à ébulition dans un tampon Laemmli contenant du DTT (un agent réducteur) pour rompre la liaison -N_3. Suivi par la migration SDS-PAGE dans un gel dénaturant, et l'excision des bandes de teneur totale en protéines qui peuvent être digérées avec de la trypsine. Les peptides obtenus peuvent être séparés et analysés par chromatographie liquide avec la base de données MASCOT pour identifier les hits de protéines et fournir le plus propre protéome de la ME de *M. xanthus*. Cela représentera une méthode révolutionnaire pour l'isolement de la ME bactérienne, qui prend d'habitude 2 jours de traitement dans une centrifugation en gradient de sucrose standard.

Ce projet aidera à élucider la capacité des bactéries à maintenir des connexions synergiques dans des environnements hétérogènes, grâce au remodelage de leurs surfaces cellulaires. L'identification de l'extrusion de la ME comme processus bactérien actif, ainsi que de tout facteur cellulaire spécifique contribuant au phénomène, permettra le développement de nouveaux agents thérapeutiques ciblés vers des protéines spécifiques et / ou des molécules responsables de la génération des structures importantes de la ME.

En conclusion, mes études ont permis la validation de l’hypothèse initial avec le développement de la méthodologie de chimie « clic », l'imagerie monocellulaire par fluorescence et l'analyse du comportement physiologique.

INDEX

FIGURE LIST

TABLE LIST

ABBREVIATIONS LIST

OM: outer membrane

IM: inner membrane

PG: peptidoglycan

OS: oligosaccharide

OMP: outer-membrane protein

LPS: lipopolysaccharide

OAg: O antigen

Lpt: lipopolysaccharide transport system

T4P: Type IV pilus

OMT: outer-membrane tube

OMV: outer-membrane vesicle

CuAAC: Cu(I)-catalyzed azide-alkyne click chemistry

SPAAC: strain-promoted azide-alkyne click chemistry

DBCO: dibenzocyclooctyne-amine

ºC: degrees Celsius

min: minutes

RPM: revolutions per minute

h: hour

1 INTRODUCTION

1.1 THE BACTERIAL CELL ENVELOPE

1.1.1 General characteristics

The bacterial cell envelope is typically structured into one of two types of arrangements, termed Gram-positive or Gram-negative, based on the capacity of the cells to retain the dye crystal violet ("positive") instead of the counter-stain safranin ("negative"). Gram-positive cells contain two layers: the inner membrane (IM) and the peptidoglycan (PG) layer **(Fig. 1)**. The former is a phospholipid bilayer that encases the cytoplasmic contents of the cell. The IM also contains lipoproteins, electrostatically-associated proteins, and integral proteins that span the biylayer via one or more α-helical transmembrane segments. The peptidoglycan (PG) cell wall sits atop the IM and constitutes a meshwork of cross-linked peptidoglycan monomers. In Gram-positive bacteria, the cell wall typically contains multiple layers of PG. Layers of PG are made up of repeating units of the dissacharide *N*-acetylglucosamine–*N*-acetylmuramic acid, which are cross-linked by pentapeptide side chains (Vollmer *et al.*, 2008). The peptidoglycan sacculus is a single very large polymer that can be isolated in its entirety, which, because of its rigidity, determines cell shape. Enteric bacteria are rod shaped, but cell shapes can vary. Agents such as enzymes or antibiotics can damage the PG causing cell lysis; without the PG, cells are more vulnerable and no characteristic shape will be present.

In Gram-negative bacteria, the cell envelope is composed of three principal layers, including an IM, an outer membrane (OM) (Zusman *et al.*), and a thin PG layer in the periplasmic space between the IM and OM. The OM is an asymmetric bilayer containing largely phospholipids in the periplasmic leaflet and the glycolipid lipopolysaccharide (LPS) in the outer leaflet (Islam & Lam, 2013) (**Fig. 1**). The OM is thus the main distinguishing compartment between Gram-negative and Gram-positive bacteria. In infections by Gram-negative bacteria, LPS from the OM is the molecule responsible for the endotoxic shock associated with septicemia. The human innate immune system is thus sensitized to this molecule because it is an indicator of infection (Whitfield, 2002). Similar to the IM, the OM also contains proteins, which can be segmented into two main classes: lipoproteins and integral membrane proteins. Lipoproteins contain lipid moieties that are typically attached to an amino-terminal cysteine residue, and it is generally thought that these lipid moieties embed lipoproteins in the inner leaflet of the OM, though cell-surface lipoproteins are becoming more widely-identified in Gram-

negative bacteria (Silhavy *et al.*, 2010). Almost every integral OM protein (OMP) assumes a β-barrel conformation, arising from sequential β sheets that circularize and adopt cylindrical forms. Many OMPs allow the passive diffusion of small molecules such as ions, amino acids, and mono/di-saccharides across the OM.

The aqueous periplasmic zone is densely packed with proteins and is more viscous than the cytoplasm (Mullineaux *et al.*, 2006). Cellular compartmentalization allows Gram-negative bacteria to sequester potentially harmful degradative enzymes such as RNAse or alkaline phosphatase in this zone. Other proteins localized to this compartment include the periplasmic binding proteins, which participate in sugar and amino acid transport and chaperone-like molecules involved in envelope biogenesis (Weski & Ehrmann, 2012). Bacteria largely lack intracellular organelles, and consequently, all of the membrane-associated functions of all typical eukaryotic organelles are performed at the IM. Most of the membrane proteins that function in energy production, lipid biosynthesis, protein secretion and transport are located in the IM (Silhavy *et al.*, 2010).

All of the components of the Gram-negative cell envelope are thus synthesized either in the cytoplasm or at the cytoplasmic leaflet of the IM. These components must be translocated from the cytoplasm or flipped across the IM. Periplasmic components must be released from the IM. Components for PG must be released and polymerized. In addition, OM components must be transported across the viscous aqueous periplasm and assembled into an asymmetric lipid bilayer. Proteins destined for the periplasm or the OM are made in a precursor form containing a signal peptide at the amino terminus, targeting them for translocation across the IM from the cytoplasm (Driessen & Nouwen, 2008).

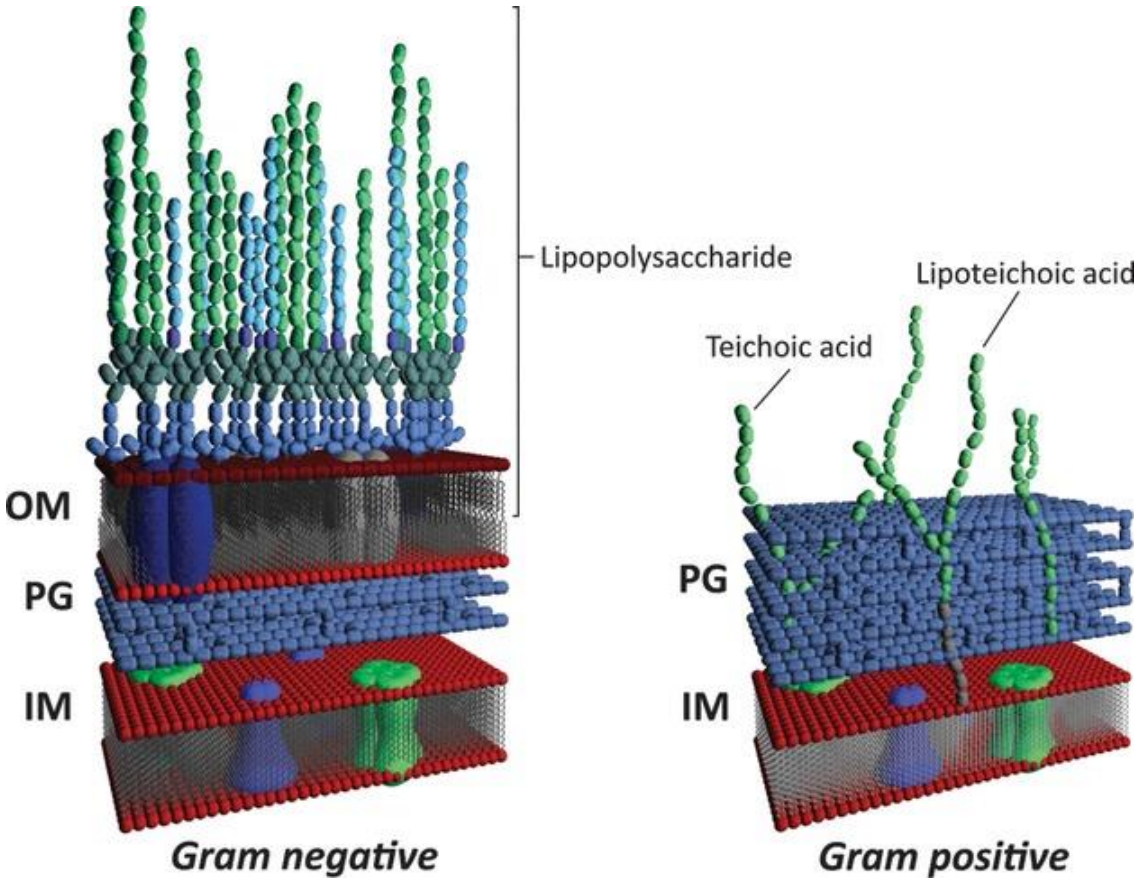

Figure 1. Cell envelope architecture in Gram-negative and Gram-positive bacteria

Membrane-spanning proteins are present in the inner membrane of both types of bacteria and are also present in the outer membrane of the latter. IM, inner membrane; PG, peptidoglycan; OM, outer membrane (Islam & Lam, 2013)

1.1.2 Role of LPS

The LPS layer plays a critical role in the barrier function of the OM. The membrane portion of LPS, known as Lipid A, is a glucosamine disaccharide with typically six or seven acyl chains. Joined to the Lipid A moiety is the core oligosaccharide (OS); this can serve as a linker region to the distal O-antigen (OAg) cap of a LPS molecule **(Fig. 2)**. The OAg is the portion of an LPS molecule that is often responsible for conferring serotyping-specificity to diverse bacterial strains. Phosphate groups linked to Lipid A on adjoining LPS molecules in the OM are typically bridged by divalent cations such as Mg^{2+}, serving to neutralize the negative charge of the phosphate groups (Bertani & Ruiz, 2018).

The acyl chains of Lipid A are largely saturated, facilitating tight packing, which imparts low fluidity and permeability to the OM. The non-fluid continuum formed by the LPS molecules is a very effective barrier for hydrophobic molecules, in addition with the diffusion of hydrophilic molecules larger than 700 Daltons by the porins, make the OM a very effective and selective permeability barrier (van den Berg, 2010).

1.1.3 Synthesis of LPS

As the LPS layer is essential for the integrity of the cellular envelope, Gram-negative bacteria need to continually replenish it in order to survive. Synthesis of LPS begins at the cytoplasmic face of the IM and follows the Raetz pathway **(Fig. 3).** For this pathway, UDP-GlcNAc and acyl-ACP are substrates required for starting Lipid A biosynthesis. LpxA, the first enzyme in the Raetz pathway, is an acyltransferase mediating the acylation of UDP-GlcNAc that yields UDP-3-(O)-acyl-GlcNAc. This reaction takes place in the cytoplasm, followed by the deacetylation of the GlcNAc moiety, which is regulated by LpxC, resulting in UDP-3-(O)-acyl-GlcN formation. As the equilibrium in the LpxA reaction is toward the substrate, the LpxC reaction is the actual step of commitment to the pathway. Once UDP-3-(O)-acyl-GlcN is formed, another acylation reaction occurs, mediated by LpxD (Vuorio & Vaara, 1995), to yield UDP-2,3-(O)-diacyl-GlcN. These three reactions take place in the cytoplasm.

Two molecules, one of UDP-2,3-(O)-diacyl-GlcN, and one of Lipid X, resulting from the removal of the UMP moiety from UDP-2,3-(O)-diacyl-GlcN, undergo Lipid A disaccharide formation. The formation of Lipid X is mediated by either LpxH or LpxI (Metzger & Raetz, 2010), depending on the bacterial species, and Lipid A disaccharide formation is mediated by LpxB. These three enzymes are peripheral IM proteins, and it appears that the reactions occur in the vicinity of the membrane.

The Lipid A disaccharide undergoes several modifications. First, the phosphorylation of Lipid A disaccharide results in the formation of lipid IVA, a tetra-acylated Lipid A species. This reaction is mediated by LpxK. Second, two 3-deoxy-D-*manno*-oct-2-ulosonic acid (Kdo) residues are attached to lipid IVA, resulting in Kdo2-IVA, and the reaction is mediated by KdtA, a Kdo transferase. The second and third reactions, mediated by LpxL and LpxM, are acylation reactions. Tetra-acylated Kdo2-IVA is transformed into Kdo2-Lipid A, the final product in the Raetz pathway. LpxL transfers lauroyl residues while LpxM transfers a myristoyl residue to Kdo2-IVA. Two reactions occur in a sequential manner: the LpxL reaction occurs before the LpxM reaction, and the LpxM reaction does not occur in the LpxL mutant (Vorachek-Warren *et al.*, 2002).

Once a molecule of LPS is synthesized on the cytoplasmic side of the IM, it is flipped to the periplasmic leaflet by the ATP-binding cassette (ABC) transporter MsbA; it is while in this leaflet that the addition of an OAg polymer may be added, mediated by the integral IM protein WaaL. LPS is then transported to the cell surface via the LPS transport (Lpt) pathway **(Fig 4).** This pathway consists of seven essential proteins, LptA, LptB, LptC, LptD, LptE, LptF, and LptG. LPS is extracted from the IM in an ATP-dependent manner by the ABC transporter LptB2FG and transferred to LptC, which forms a complex with LptB2FG. LptC consists of a single membrane-spanning domain and a large periplasmic domain, which forms a periplasmic bridge with the soluble protein LptA and the amino-terminal region of LptD. LPS transverses the aqueous periplasmic space through this protein bridge and reaches the cell surface with the aid of the carboxy-terminal domain of LptD, which forms a β-barrel structure that is plugged by the OM lipoprotein LptE (Okuda *et al.*, 2016).

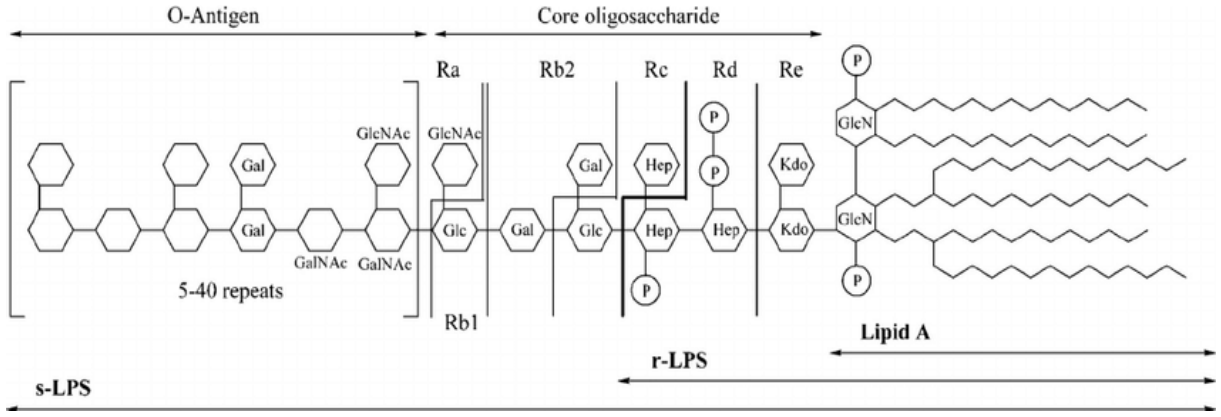

Figure 2. Structure of a LPS molecule from *E. coli*

Gal, galactose; GalNAc, N-acetyl-galactosamine; Glc, glucose; GlcN, glucosamine; GlcNAc, N-acetyl-glucosamine; Kdo, 2-keto-3-deoxyoctonic acid; Hep, L-glycerol-D-manno-heptose ; S-LPS (smooth LPS), composed of O-antigen (O-Ag), complete core oligosaccharide, and lipid A; r-LPS, (rough LPS) lacks O-Ag, possesses lipid A and progressively shorter core oligosaccharides. (Bagheri *et al.*, 2011).

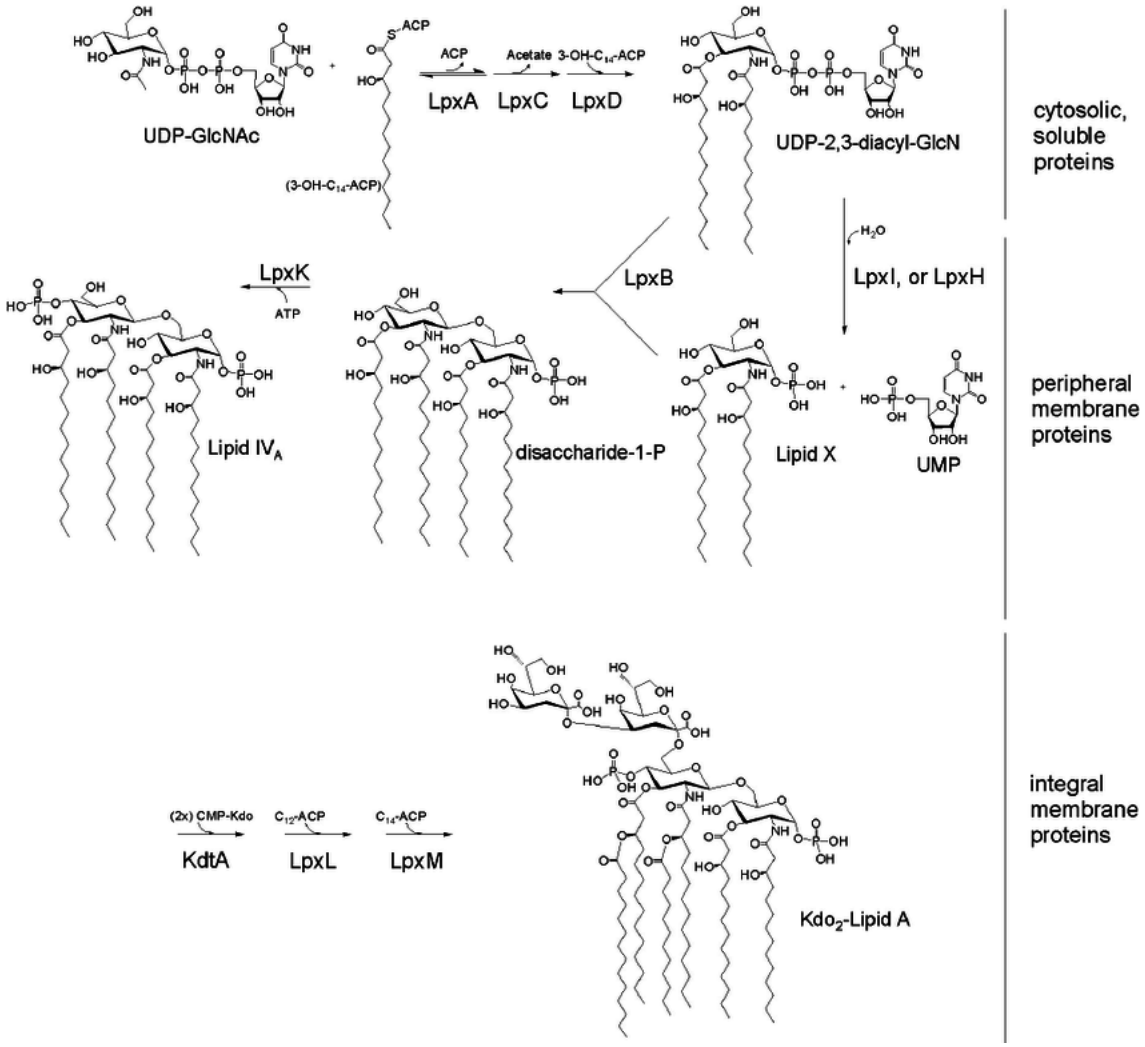

Figure 3. Synthesis of LPS via the Raetz pathway

Constitutive enzymes of Lipid A biosynthesis (Joo, 2015).

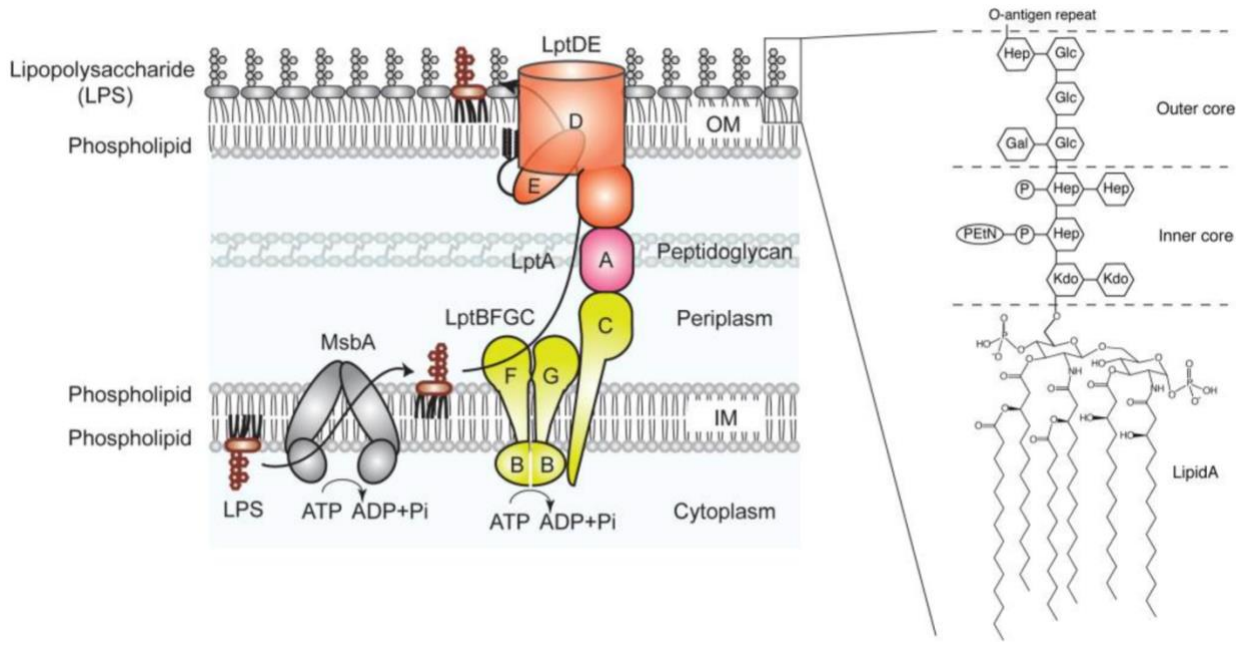

Figure 4. Transport of LPS via the Lpt pathway

The Lpt system extracts LPS from the periplasmic leaflet of the IM and provides energy to drive LPS across the Lpt bridge through an ATPase-dependent mechanism. Once across the periplasm, LPS is inserted laterally into the outer leaflet of the OM where it is dispersed across the cell surface (Okuda *et al.*, 2016).

1.2 *MYXOCOCCUS XANTHUS*

1.2.1 Physiology of *Myxococcus xanthus* (myxobacteria)

Myxobacteria are characterized by a rich social lifestyle **(Fig. 5)**. These social interactions play decisive roles in growth, motility and development and allow myxobacterial cells to organize into distinct spatial patterns as well as to feed cooperatively. *Myxococcus xanthus* has emerged as the pre-eminent model system to understand the genetics and molecular mechanisms involved in the social behavior of myxobacteria and more broadly in the evolution of multicellularity in higher organisms (Velicer & Yu, 2003).

Myxococcus xanthus belongs to the "delta" class of proteobacteria. Myxobacteria are found throughout the environment (Wang *et al.*, 2011) and have predatory capacities when in the presence of prey microorganisms. The social lifestyle of *M. xanthus* crucially depends on the ability of cells to display active movement. If present on a solid surface and at a high cell density*, M. xanthus* cells self-organize into three morphologically distinct spatial patterns, spreading colonies, ripples or fruiting bodies. The pattern formed largely depends on the nutritional status of the cells. In the presence of nutrients, the motile, rod-shaped cells grow and divide and form spreading colonies. Cells at the edge of a colony spread coordinately over the surface, forming a thin, film-like structure. In the absence of nutrients, the spreading behavior is constrained and cells initiate a developmental program that culminates in the formation of multicellular, spore-filled fruiting bodies (Zusman *et al.*, 2007) **(Fig. 5)**.

1.2.2 Motility systems of *M. xanthus*

M. xanthus moves on surfaces by using two complementary flagella-independent motility forms: single-cell gliding (adventurous [A]) motility and Type IV pilus (T4P)-dependent (social [S]) motility. Both motility systems, coordinated in space and time, not only facilitate the surface movement of individual cells, but are also essential for the expansion of multicellular swarms, predation and construction of multicellular fruiting bodies (Nan & Zusman, 2011). Gliding motility drives the movement of single cells at the swarm edges; such cells glide slowly to explore new environments, change direction through reversal events, and leave behind slime trails that may be followed by other cells. Cells undergoing gliding utilize bacterial focal adhesions to power movement. In these cells, the trans-envelope gliding transducer (Glt) complex, powered by the proton motive force-driven AglRQS motor, is helically transported within a cell; once this complex becomes adhered to the substratum, continued motorized transport of the fixed

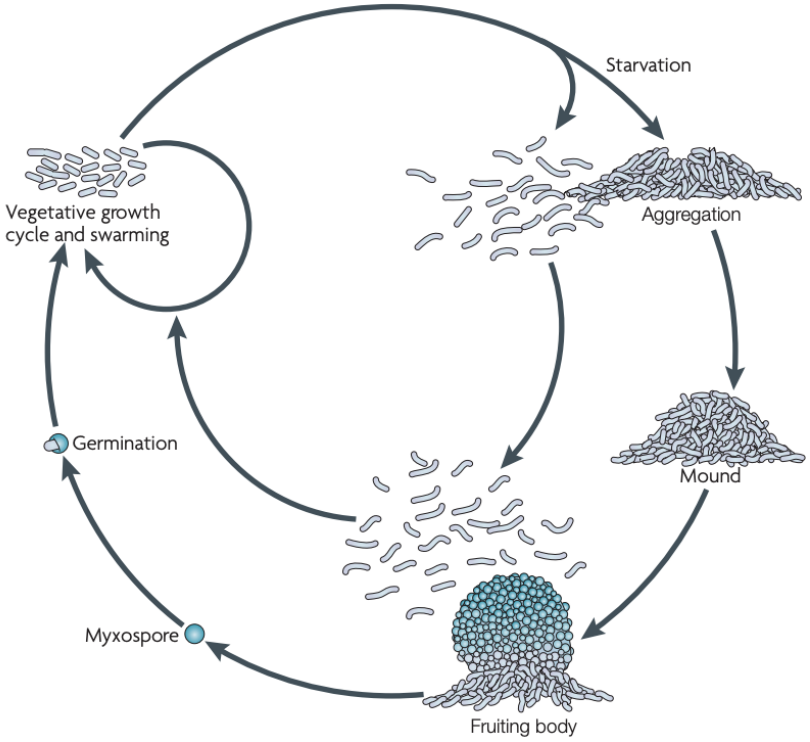

Figure 5. Lifecycle of *Myxococcus xanthus*

When nutrients are present, groups of cells (swarms) grow and divide and move outward in search of additional macromolecules or prey. Upon starvation, cells aggregate forming mounds and fruiting bodies. When nutrients become available, the spores germinate and complete the life cycle (Zusman et al., 2007)

(relative to the substratum) Agl–Glt complex results in forward propulsion of the cell (Islam & Mignot, 2015; Islam, *et al.,* 2020). Gliding motility in *M. xanthus* is associated with the deposition of a poorly-characterized “slime” polysaccharide trail behind cells on hard surfaces, which may serve to increase substratum adherence of the Agl–Glt complex and potentially serve as a path to follow for subsequent cells (Ducret *et al.*, 2012).

T4P-dependent motility is characterized by the movement of large cell groups and is stimulated by cell–cell proximity. This motility is crucial for both fruiting body formation and cooperative predation. In addition to T4P appendages, two polysaccharides are required for this type of motility. The presence of the specific cell-surface exopolysaccharide (EPS) polymer is required for binding of the T4P from an adjacent cell (Lu *et al.*, 2005). However, this surface-associated EPS appears to require functional activation by secreted biosurfactant polysaccharide (BPS) before T4P-dependent group motility and swarm expansion can take place (Saidi et al. 2020).

1.2.3 OM dynamics

The *M. xanthus* OM displays dynamic properties that impact the complex physiology of the bacterium. Within multi-cell biofilms, cells of *M. xanthus* were shown to be connected via networks of OM vesicle (OMV) chains and OM tube (OMT) projections (Remis *et al.*, 2014). Individual OMV and zipper-like structures have also been reported; these OMVs were either in direct contact with the OM of intact cells or were linked to the OM of intact cells by putative proteinaceous tethers. Occasionally, individual OMVs were also connected by potential proteinaceous tethers showing features consistent with the presence of cargo or an internal organization. In areas in which two cells were in direct contact, zipper-like structures were observed connecting the OMs. These zipper-like structures often showed accumulation of material that is most likely of a proteinaceous nature (Palsdottir *et al.*, 2009).

In myxobacteria, the recognition of compatible receptors leads to outer membrane exchange among clonemates and fitness consequences (Cao & Wall, 2017). OM protein exchange is not restricted to motility proteins and virtually any OM protein and even lipid can be exchanged between cells. Gliding motility has been shown to be important for transfer, but rather indirectly by promoting the formation of dense regions of aligned cells and favoring intimate cell–cell contacts.The transfer process itself depends on two specific proteins, TraA and TraB (Pathak *et al.*, 2012) . TraA is a protein with hallmarks of yeast floculins, a class of cell surface adhesins that mediate cell–cell interactions leading to flocculation (Smukalla *et al.*, 2008). TraB is a secreted protein of unknown function with a possible peptidoglycan-binding

domain. Compatible TraA and TraB proteins must be expressed both by donor and recipient cells for transfer to occur.

Ducret and colleagues observed that contact between two cells on a solid surface was sufficient to stimulate transfer of proteins and lipids between the fused OM compartments. But not all contacts led to a transfer. Importantly, when cells that had swapped fluorescent membrane components moved apart, they appeared to remain connected by tubular structures, suggesting that an inter-OM junction must have formed to allow proteins and lipids to be transferred between the cells. This junction is referred to as an OM synapse **(Fig. 6A)** (Ducret *et al.*, 2013)**.**

Independently, OMT-like structures were also shown to be produced at surprisingly high levels when cells were grown in liquid medium without agitation. These OM-derived structures were long and exceeded multiple cell lengths **(Fig. 6B)**. When viewed via transmission electron microscopy, the morphology of these OM-derived extrusions varied between tubes and chain-like structures. Intermediate-like structures are also found, suggesting that OMTs may transition between these two morphotypes (Wei *et al.*, 2014a).

Given the dynamic nature of the *M. xanthus* OM, deeper mechanistic insights into the various processes described above require methods to specifically visualize and analyze this cellular compartment.

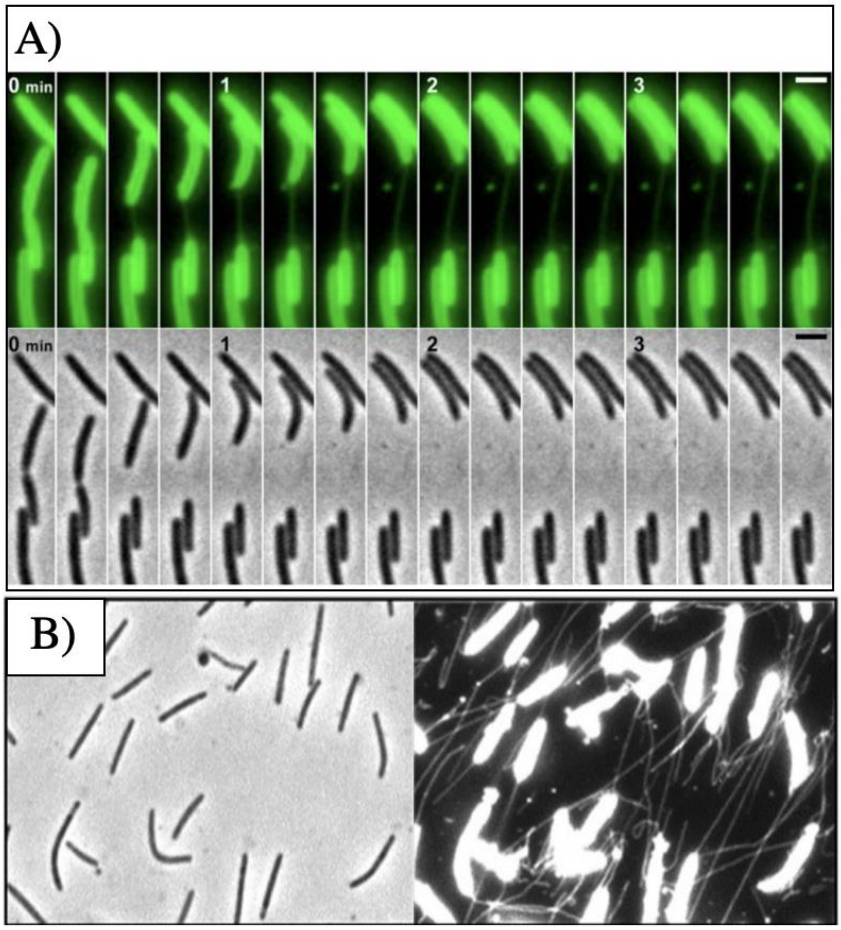

Figure 6. Types of OMTs formed by *M. xanthus*

(A) OMTs formed between cells expressing OM_{sfGFP} with fused OM layers due to gliding in opposite directions on a solid substratum (Ducret *et al.* 2013). **(B)** *Left panel:* During phase-contrast imaging, no OM cell-cell conections are seen. *Right panel:* Fluorescence imaging of these same cells prevously stained with DilC fluorescent dye reveals distinct inter-cell OM connections (Wei *et al.*, 2014a).

1.2.4 Partial structure of *M. xanthus* LPS from strain DK1622

The reference strain *Myxococcus xanthus* DK1622 produces a smooth-type LPS. The structure of the OAg and the Lipid A–core OS regions of the LPS were determined by chemical and spectroscopic methods (Maclean *et al.*, 2007) **(Fig. 7A)**, with the OAg shown to be composed of repeating disaccharide units with the following structure:

→6)-α-D-Glcp-(1→4)-α-D-GalpNAc6OMe∗-(1→

The GalNAc residue was found to be partially methylated. The core OS consisted of a phosphorylated hexasaccharide, containing one Kdo residue, unsubstituted at O-4, and no heptose residues. The Lipid A component consisted of β-GlcN-(1→6)-α-GlcN1P disaccharide, N-acylated with 13-methyl-C_{14}-3OH (*iso*-C_{15}-3OH), C_{16}-3OH, and 15-methyl-C_{16}-3OH (*iso*-C_{17}-3OH) acids.

The lipid portion was found to contain O-linked *iso*-C_{16} acid **(Fig. 7B)**; however, remaining acyl chains were not detected in this analysis, suggesting that they may be O-linked (Maclean *et al.*, 2007). Interestingly, the detected acyl chains were found to be branched, a rare occurrence for Lipid A acyl chains, a characteristic otherwise only detected in *Bacteroides fragilis* (Lindberg *et al.*, 1990) and *Porphyromonas gingivalis* (Jain & Darveau, 2010). The significance of this branching remains to be determined.

1.2.5 OM labelling via genetically-encoded fluorescent proteins

One method for OM labelling for live-cell imaging of bacteria is by genetically-encoded fluorescent proteins. Over the past two decades, genetically encoded fluorescent tags have revolutionized cell biology. These are protein sequences that fold and become fluorescent either by formation of a fluorophore from the protein sequence or by binding a small-molecule fluorophore. Intensive engineering of these proteins has led to a large variety of tags, with diverse fluorescent emission spectra, that enables multicolor imaging of target proteins by genetically fusing the fluorescent tag coding sequence to the gene of interest. When paired with modern microscopy techniques, this provides a powerful way to interrogate biological processes of interest. A key feature of fluorescent proteins is that they are genetically encoded and thus can be used to label proteins in live cells with absolute specificity; absent proteolysis, fluorescent proteins thus colocalize with the fusion protein they were designed to study. In addition, fluorescent proteins are highly stable, and the chromophore is sheltered by the protein's barrel structure, making fluorescent proteins ideal reagents to track the localization and movement of fusion proteins in cells (Thorn, 2017). Nevertheless, there are certain

disadvantages presented by this methodology. The overall bulk of conventional fluorescent proteins has the potential to interfere with the target protein's localization, structure, or activity, especially if the target is of a smaller size than the tag. Despite efforts to modulate the environmental sensitivity of fluorescent proteins, the barrel structure isolates the chromophore from the cellular environment making fluorescent proteins poor probes for environmental cues like pH, hydrophobicity and ion concentrations (Marks & Nolan, 2006).

In *M. xanthus*, both super-folder green-fluorescent protein (sfGFP) and mCherry have been successfully used to label the OM. This was accomplished by expression of either sfGFP or mCherry with a N-terminal lipoprotein sorting signal to target the fusion protein to the periplasmic leaflet of the OM (OMss-sfGFP and OMss-mCherry, respectively), resulting in fluorescent labelling of the cell periphery (Ducret *et al.*, 2013). In this report, outer-membrane exchange studies were performed using these OM-targeted fluorescent constructs. One technical limitation to the use of OM-labelling constructs such as these is that the specific cellular compartment being labelled is the predominantly phospholipid-containing periplasmic leaflet of the OM; labelling of the surface leaflet of the OM, largely composed of LPS, does not occur.

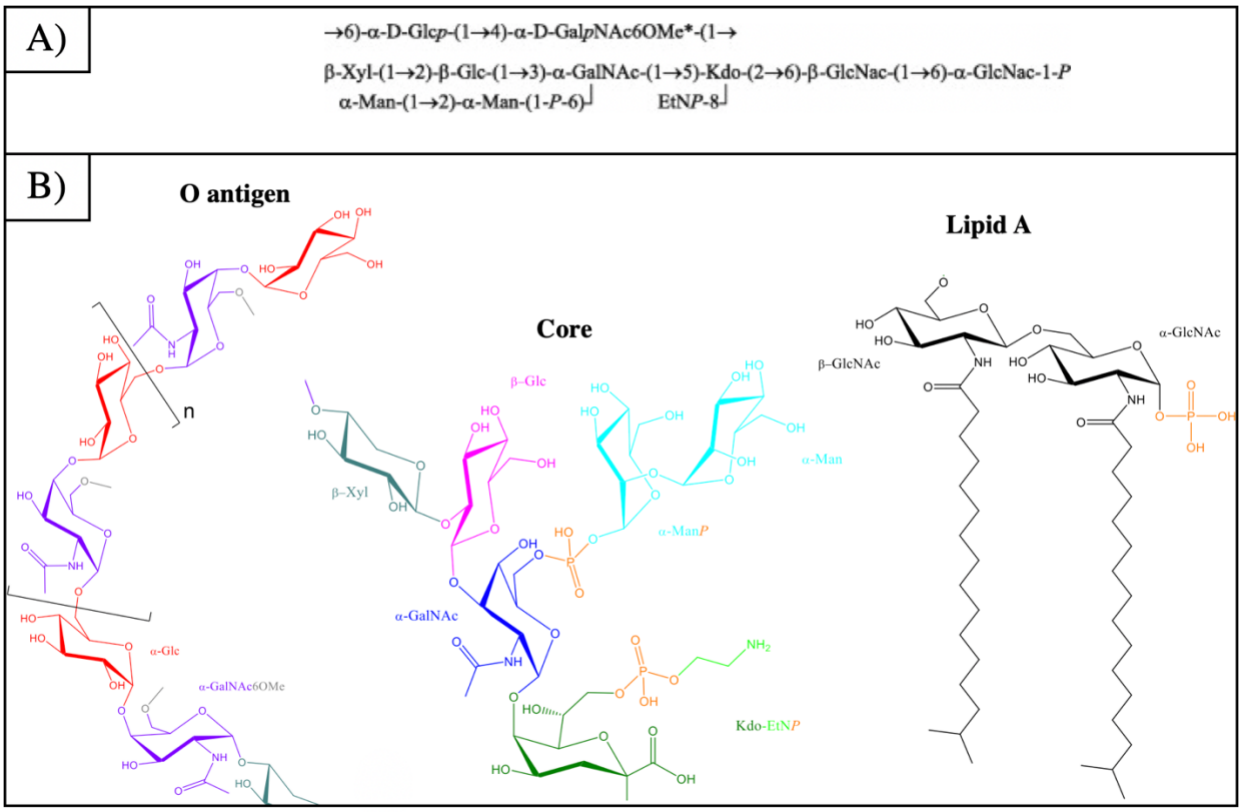

Figure 7. Structure of *M. xanthus* DK1622 LPS

(A) Chemical structure of O Ag and Lipid A– core OS segments (Maclean et al. 2007). **(B)** Separate diagrammatic representation of O Ag, core OS, and Lipid A sections of *M. xanthus* DK1622 LPS (S.T. Islam, *unpublished, used with permission).*

1.2.6 OM labelling via fluorescent dyes

Alternatively, fluorescent lipophilic dyes have also been used to successfully label the OM of bacteria. Specifically, two lipophilic dyes have been successfully used to label *M. xanthus* cells. The first is DiO, a hydrophobic fluorescent lipid dye (containing a C_{18} backbone), that can be added directly to normal culture media to uniformly label suspended or attached culture cells for use in cell-cell fusion, cellular adhesion and migration applications (ThermoFisher, 2020) (Ducret *et al.*, 2013) . The second dye used is DiIC (Wei *et al.*, 2014b), a similar lipophilic dye that diffuses laterally in a membrane to stain the entire cell. It is weakly fluorescent until incorporated into membranes, it is spectrally similar to tetramethylrhodamine, and it is often used as a long-term tracer for neuronal and other cells. Both dyes and their multiple variants are significantly attractive in the field since they do not appreciably affect cell viability, development, or basic physiological properties of the cells and/or molecules in which they are used (Atwal *et al.*, 2016).

A different staining method was reported to be a possible alternative for OM staining targeting the LPS in the outer-leaflet of the OM (polymyxin B-BODIPY FL), a fluorescent conjugate of polymyxin B (Wei *et al.*, 2014b). Polymyxin B is a cationic lipopeptide antibiotic which binds specifically to Gram-negative bacteria.

1.3 CLICK CHEMISTRY

"Click" chemistry can be defined as a series of reactions that are (i) high yielding, (ii) wide in scope, (iii) create only byproducts that can be removed without chromatography, (iv) are stereospecific, (v) simple to perform, and (vi) can be conducted in benign solvents. This concept was developed in parallel with the interest within the pharmaceutical, materials, and other industries in capabilities for generating large libraries of compounds for screening in discovery research. Several types of reactions have been identified that fulfill these criteria. These include thermodynamically-favored reactions that lead specifically to one product, such as nucleophilic ring opening reactions of epoxides and aziridines, non-aldol type carbonyl reactions, such as formation of hydrazones and heterocycles, additions to carbon-carbon multiple bonds, such as oxidative formation of epoxides, and cycloaddition reactions (Kolb *et al.*, 2001). The main characteristics that click chemistry technology offers are:

- It is highly selective methodology, with low background labeling: Click functional groups are inert to naturally occurring functional groups ("bioorthogonal") such as amines.
- Rapid and quantitative labeling.
- It allows non-radioactive analysis of enzymatic activities both *in vitro* and *in vivo*.

1.3.1 Types of click-chemistry reactions

Click Chemistry reactions can be categorized into two separate groups: copper (Cu(I))-catalyzed and copper-free. The Cu(I)-catalyzed azide-alkyne cycloaddition (CuAAC) click chemistry reaction relies on the presence of Cu(I) ions whereas the copper-free strain-promoted azide-alkyne cycloaddition (SPAAC) click chemistry reaction and the tetrazine–alkene ligation efficiently proceeds without metal catalysts. The copper-free azide-alkyne reaction is hampered by the instability of alkynes and slow reaction kinetics. Recent focus therefore shifted towards strain-promoted reactions with cyclooctynes and tetrazine–alkene ligation, respectively (Hein *et al.*, 2008).

1. Cu(I)-catalyzed azide-alkyne cycloaddition (CuAAC) reaction **(Fig. 8)**:

Since terminal alkynes are fairly unreactive towards azides, the efficiency of a CuAAC reaction strongly depends on the presence of a metal catalyst such as copper (Pathak *et al.*) in the +1-oxidation state (Cu(I)). Different copper sources and reducing reagents are available; however, the Cu(II) salt $CuSO_4$ as copper source in combination with ascorbate as a reducing reagent has been recommended for most biomolecular labeling applications. However, the use

of CuAAC reactions in live cells is hampered by the toxicity of Cu(I) ions (Himo *et al.*, 2005). It is interesting to note that, in contrast to non-catalyzed alkyne-azide cycloadditions performed using heat, CuAAC reactions are regioselective and lead to the formation of only one of the two possible isomers (Hein *et al.*, 2009).

2. Strain-promoted azide-alkyne cycloaddition (SPAAC) reaction **(Fig. 9)**:

The requirement of a cytotoxic copper catalyst often limits the usage of CuAAC reactions, as it is not conducive to live-cell imaging. Conversely, a copper-free and thus non-toxic labeling method of azides is the strain-promoted azide-alkyne cycloaddition (SPAAC) reaction. SPAAC reactions rely on the use of strained cyclooctynes that possess a remarkably decreased activation energy in contrast to terminal alkynes and thus do not require an exogenous catalyst. A number of structurally varied cyclooctyne derivatives e.g. Difluorocyclooctyne (DIFO), Bicyclononyne (BCN), Dibenzoazacyclooctyne (DIBAC), Dibenzocyclooctyne (DIBO), Azadibenzocyclooctyne (ADIBO), have been developed that strongly differ in terms of reaction kinetics. (Takayama *et al.*, 2019).

A major shortcoming of SPAAC is that the degree of regioselectivity in the transition state of the reaction is usually low, resulting in the formation of isomeric products (Gröst & Berg, 2015).

3. Tetrazine-alkene ligation **(Fig. 10)**:

The tetrazine-alkene ligation constitutes a non-toxic biomolecule labeling method of unparalleled speed that is ideally suited for *in vivo* cell labeling and low concentration applications. A number of structurally-varied alkene and tetrazine derivatives have been developed that strongly differ in terms of reaction kinetics and stability. Trans-cyclooctene (TCO) has been selected since it possesses the highest reactivity towards tetrazine. Methylcyclopropene and Vinyl (terminal alkene) possess excellent substrate properties for enzymatic applications due to their small size (Kang *et al.*, 2016).

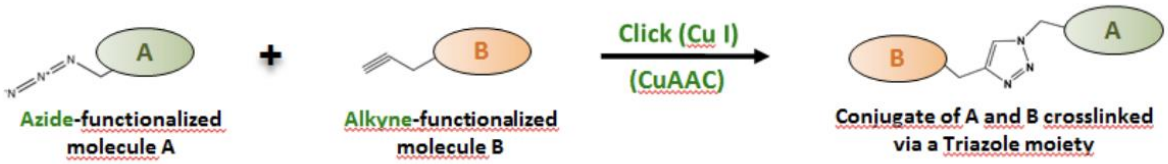

Figure 8. Principle of Cu(I)-catalyzed azide-alkyne cycloaddition (CuAAC)
An azide-functionalized molecule A reacts with a terminal alkyne-functionalized molecule B thereby forming a stable conjugate A-B in presence of a copper catalyst via a triazole moiety (Sharpless, 2002).

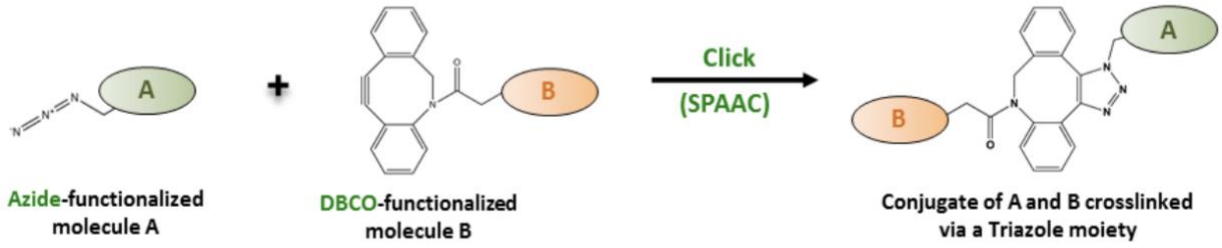

Figure 9. Principle of strain-promoted azide-alkyne cycloaddition (SPAAC)
An azide-functionalized molecule A conjugates with a dibenzocyclooctyne (DBCO) resulting in the crosslinked conjugated via triazole moiety (Bertozzi *et al.*, 2004) .

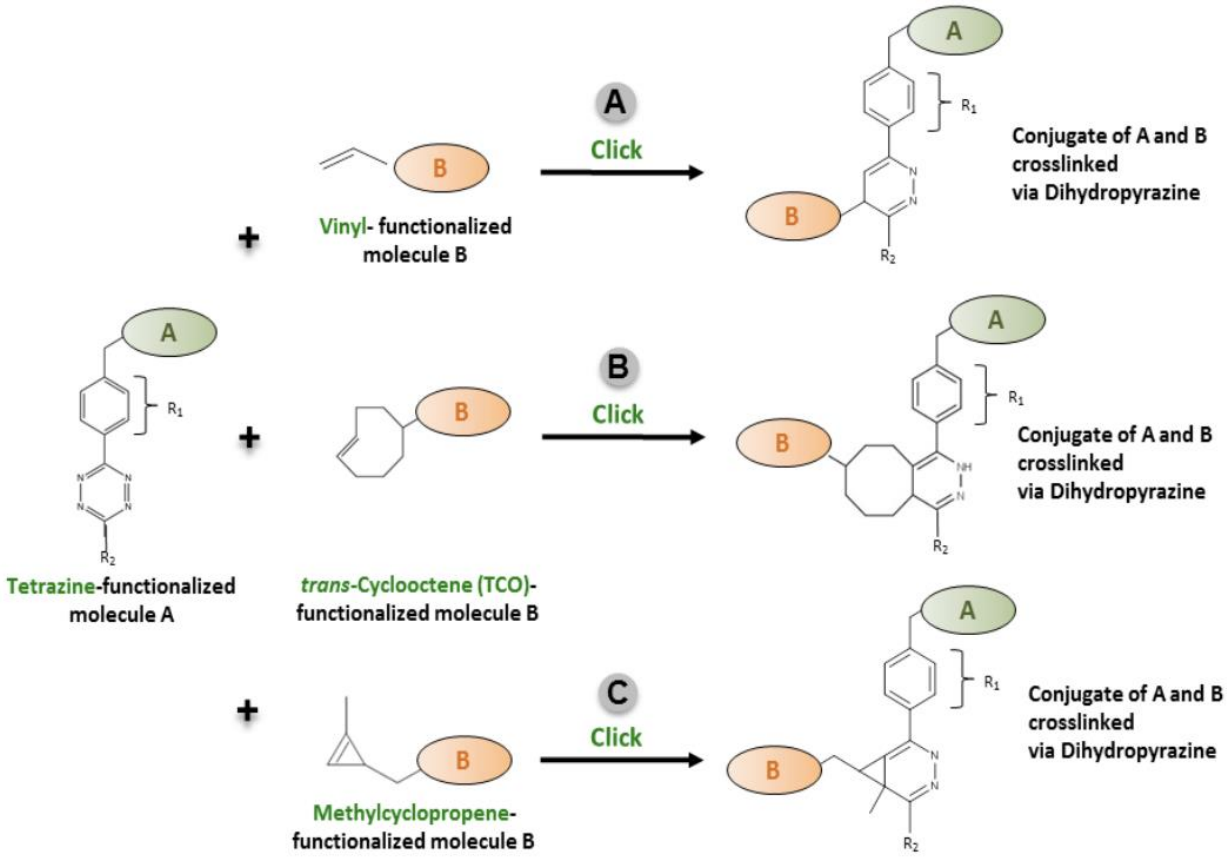

Figure 10. Principle of tetrazine-alkene ligation

Tetrazine-functionalized molecule A reacts with a terminal or stained alkene-functionalized molecule B forming a stable conjugate A-B. **A)** Tetrazine-Vinyl Ligation. **B)** Tetrazine-trans-Cyclooctene Ligation. **C)** Tetrazine-Methylcyclopropene Ligation (Selvaraj & Fox, 2013).

1.4 CLICK-CHEMISTRY TECHNOLOGY USES

Click chemistry describes pairs of functional groups that rapidly and selectively react ("click") with each other under mild, aqueous conditions. The concept of click chemistry has been transformed into convenient, versatile and reliable two-step coupling procedures of two molecules A and B that are widely used in biosciences, drug discovery and material science (Nwe & Brechbiel, 2009); For example:

- On DNA
    - Enzymatic click-functionalization of DNA
- On RNA
    - Global RNA synthesis monitoring
- On Proteins
    - Protein synthesis monitoring (Site and residue selective)
- On Bacteria
    - Gram-negative bacteria cell-surface labelling

1.5 METABOLIC LABELLING USING KDO-N_3 AND CLICK CHEMISTRY

Kdo-N_3 is a synthetic variant of 3-deoxy-D-*manno*-oct-2-ulosonic acid (Kdo) **(Fig. 11)**, with the latter already known to be an essential component of LPS in the outer leaflet of the Gram-negative bacterial OM **(Fig. 7)**. For the synthetic Kdo-N_3 sugar, the -N_3 modification has been introduced at position 8 of the sugar molecule **(Fig. 11)** (Nilsson *et al.*, 2017), with this motif allowing for OM labeling by click-chemistry reactions. In WT *M. xanthus* cells, this position of the Kdo sugar in a native LPS molecule is modified with a phosphoethanolamine (PEtN) moiety **(Fig. 7)**.

Metabollic incorporation of the Kdo-N_3 molecule has been used as a novel technology for probing both eukaryotic and prokaryotic physiology. Thusfar, the use of Kdo-N_3 in research has been focused on labelling various physiological structures that normally contain Kdo, something that is applicable to both eukaryotes and prokaryotes.

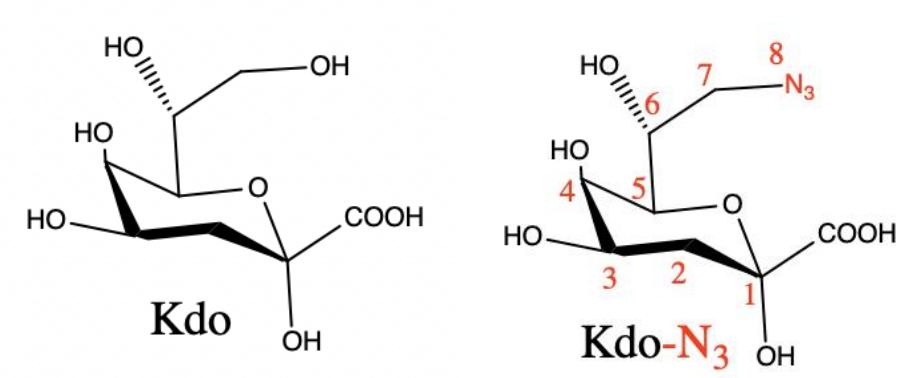

Figure 11. Chemical structure of Kdo vs. Kdo-N_3

Kdo-N_3 presents the click-chemistry motif N_3 in the 8^{th} carbon of the molecule being the difference between the two structures.

1.6 METABOLIC LABELING OF THE *ARABIDOPSIS THALIANA* CELL WALL

Kdo-N_3 technology has been used in plants and bacteria for labelling purposes. In plants, Kdo **(Fig. 11)** is only found in the cell wall pectin, rhamnogalacturonan-II (RG-II). Dumont et al. incubated 4-day-old light-grown *Arabidopsis* seedlings with Kdo-N_3 followed by coupling to an alkyne-containing fluorescent probe resulted in the specific in muro labelling of RG-II through a CuAAC reaction **(Fig. 12A)**.

CMP-Kdo synthetase inhibition and competition assays were performed and reflected that Kdo and D-Ara, a precursor of Kdo, inhibit Kdo-N_3 incorporation demonstrating that the incorporation of Kdo-N_3 occurs in RG-II through the endogenous biosynthetic machinery of the cell. Co-localisation of Kdo-N3 labelling with the cellulose-binding dye calcofluor white demonstrated that RG-II exists throughout the primary cell wall. Additionally, after incubating plants with Kdo-N_3 and an alkynated derivative of L-fucose that incorporates into rhamnogalacturonan I, co-localized fluorescence was also observed in the cell wall at the elongation zone of the root. Finally, Ducret *et al.* perfomed pulse labelling experiments that demonstrate that metabolic click-mediated labelling with Kdo-N_3 provides an efficient method to study the synthesis and redistribution of RG-II during root growth (Dumont *et al.*, 2016).

1.7 METABOLIC LABELLING OF THE GRAM-NEGATIVE OUTER MEMBRANE

Similar labelling work has been done in *Escherichia coli* **(Fig. 12B)** by Dumont et al., where non-pathogenic *E. coli* K12, which lacks an OAg, was cultured overnight in the presence of Kdo-N_3, then treated with an Alexa Fluor 488 fluorophore conjugated to a terminal alkyne group under optimized CuAAC copper-catalyzed click reaction conditions. After incubation under these click reaction conditions, the bacteria were labeled very brightly, whereas control experiments in the absence of Kdo-N_3 did not generate any significant fluorescence. The fluorescence signal was detected around the cell periphery, suggesting that the cell-surface LPS had been selectively labeled as expected. (Dumont *et al.*, 2012).

After localizing the fluorophore to the OM, Kdo-N_3 incorporation into the LPS molecule itself was first validated on a molecular level using SDS-PAGE. *E. coli* cells were grown in the presence/absence of Kdo-N_3, followed by reaction with Alexa488-DIBO and LPS separation by SDS-PAGE. Fluorescence scanning revealed a green fluorescent band in the sample from cells grown with Kdo-N_3 and treated with Alexa488-DIBO **(Fig. 13A).** This band was not detected in control samples: untreated cells, cells grown without Kdo-N3 and treated with Alexa Fluor-488-DIBO, and cells grown with Kdo-N_3 but untreated with Alexa488-DIBO (Nilsson *et al.*, 2017).

In order to have a direct read-out of Kdo-N_3 without the competition of endogenous Kdo present in *E. coli* K12 that is incorporating into the LPS, Nillson *et al.* used an *E. coli* strain (ClearColi K-12) that presented a lack of endogenous Kdo synthesis but retains intact Kdo cytidylyltransferase (CMP-Kdo synthetase, KdsB, or CKS). It is also shown that ClearColi K-12 synthesizes only lipid IV_A as its LPS. Nillson *et al.* tested the hypothesis that this strain should be capable of synthesizing core-lipid IV_A after uptake of exogenous Kdo or exogenous Kdo-N_3, by growing ClearColi K-12 in the presence of 5 mm Kdo-N_3 for 16 h followed by the reaction with Alexa488-DIBO. After SDS-PAGE and LPS staining a band equivalent to rough LPS (core-lipid IV_A) was clearly visible from ClearColi K-12 grown with Kdo. Followed the SDS-PAGE results indicating Kdo-N_3 incorporation into the LPS, the total lipid extracts were analyzed by MALDI-TOF MS, a low-intensity signal was observed at m/z 1623.83 in both samples, which can be interpreted as Kdo-lipid IVA. MS/MS fragmentation of this ion led also to m/z 1403.8, indicating the loss of one Kdo unit to form lipid IV_A. A peak at m/z 1843.96, which would be consistent with $(Kdo)_2$-lipid IV_A, was not observed. Whereas ClearColi K-12 is reported to lack the ability to synthesize Kdo, these results confirmed the presence of Kdo-N_3–lipid IV_A (Nilsson *et al.*, 2017).

Subsequently, Nillson et al. show that the sialic acid transporter NanT in *E. coli* is responsible for the uptake of exogenous Kdo and Kdo-N_3 into the cytoplasm where core-LPS biosynthesis takes place. While the *nanT* knockout strain of *E. coli* did not show any fluorescent labeling, restoring NanT expression enhanced Kdo-N_3 incorporation and fluorescent labeling.
The IPTG-induced NanT expression also increased Kdo uptake and incorporation in ClearColi, an *E. coli* K-12 derivative strain that lacks endogenous Kdo biosynthesis. While Kdo supplementation restored Lipid A + core OS biosynthesis, bypassing the existing mutations in the strain, Kdo-N_3 supplementation only partially restored full-length core-LPS along with significant amounts of truncated LPS (Nilsson et al., 2018). As an example of existing uses of Kdo-N_3 metabolic labelling in bacteria, Fugier and colleagues developed an innovative technology; via cell tagging through non-lethal click chemistry (SPAAC) and sorting with dynabeads M-280 streptavidin (Invitrogen) magnetic beads, click-able *E. coli* cells could be rapidly detected, enriched and concentrated from a mixture containing also *Bacillus subtilis* present (with *E. coli* and *B. subtilis* used as model organisms containing or lacking Kdo, respectively). This technology can be used in various diagnostic areas like environmental, biological or food processing controls since it is necessary to determine the potential presence of a set of bacteria of interest (Fugier et al., 2015).

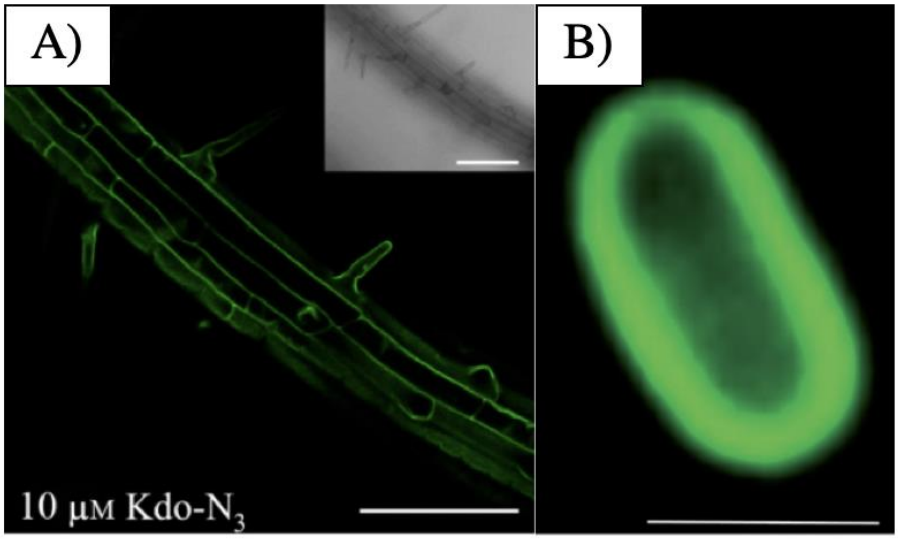

Figure 12. SPAAC-mediated *in vivo* labelling of organisms

A) Confocal microscope images of roots from *Arabidopsis thaliana* seedlings SPAAC- mediated labelling with fluorescent Alexa Fluor 488, scale bar = 10 µm. Insert corresponds to the transmitted light image (Dumont *et al.*, 2016) . **B)** *E. coli* K12, grown in the presence of Kdo-N_3, SPAAC-labelled with fluorescent Alexa Fluor 488 (A488-yne), scale bar = 1 µm (Dumont *et al.*, 2012).

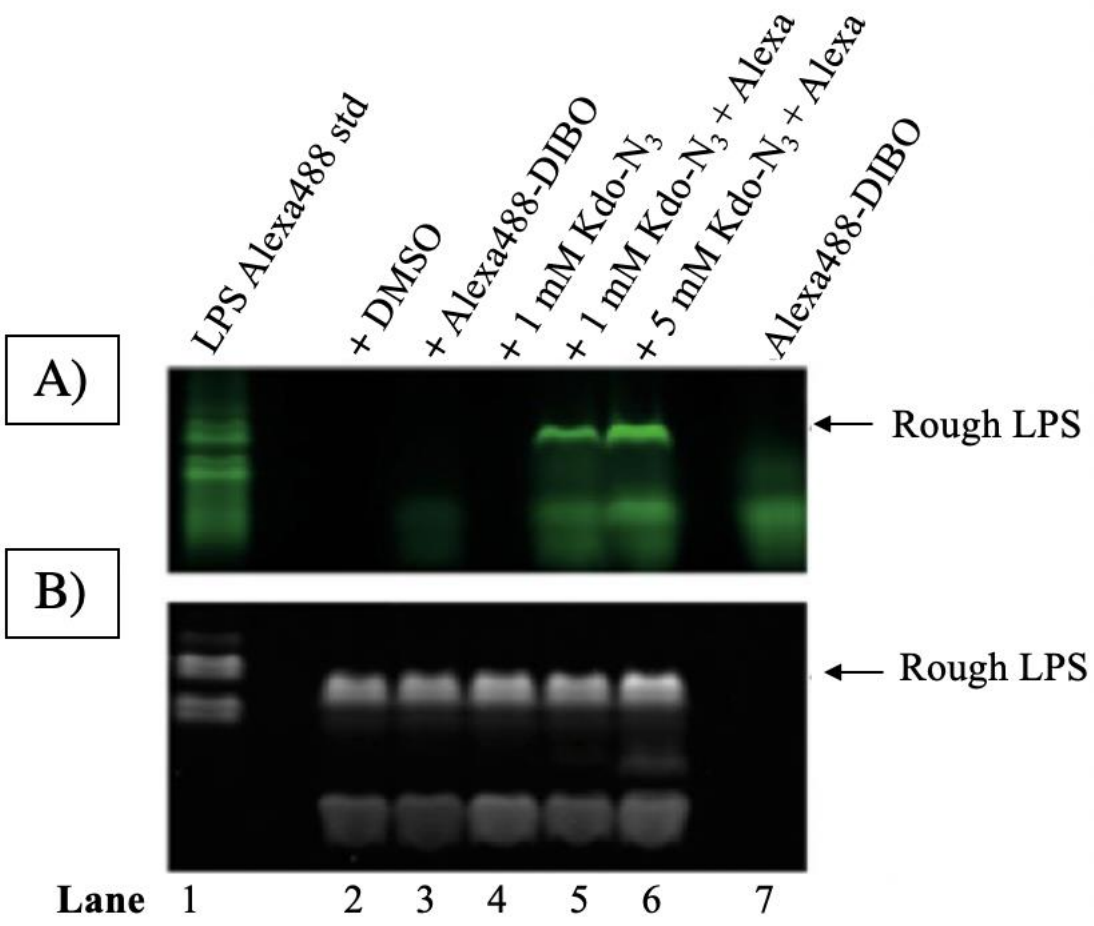

Figure 13. Incorporation of Kdo-N_3 into LPS of *E. coli* K-12

E. coli K-12 was grown in LB with and without 1 mm or 5 mm Kdo-N_3, respectively, and fluorescently labeled with AlexaFluor488-DIBO. LPS was reseolved via SDS-PAGE. **A)** SDS-PAGE image of *E. coli* K-12 visualized by fluorescent imaging for Alexa Fluor 488. **B)** SDS-PAGE image of *E. coli* K-12 after Pro-Q Emerald 300 LPS staining kit. (Nilsson *et al.*, 2017).

2 RATIONALE

Remodelling of the bacterial cell surface is a ubiquitous phenomenon for maintaining connections with the substratum and/or other cells, thus facilitating communication, behavioral coordination, and long-term residence. Given its complex social lifestyle, the Gram-negative δ-proteobacterium *M. xanthus* has become the model system in which to study OM-dependent interactions in bacteria. Upon nutrient starvation, single gliding cells and motile cell groups (powered by collective extension and retraction of Type IV pili) assemble into an aggregate, which eventually matures into a spore-filled fruiting body. Within *M. xanthus* aggregates, cells become connected to each other via networks of OM-derived tubes (OMTs) and vesicle (OMV) chains composed of LPS. OMVs are ubiquitous in Gram-negative bacteria and implicated in communication, nutrient digestion, and toxin delivery (Haurat *et al.*, 2015); however, the mechanism of OM extrusion in general is poorly understood. Before this process can be studied in real time, a method to specifically label the LPS on the surface of *M. xanthus* cells is required.

I hypothesize that the M. xanthus OM can be successfully metabolically labelled via Kdo-N_3 uptake and incorporation into nascent LPS, followed by click chemistry-based fluorescence functionalization of cell-surface LPS elaborating Kdo-N_3. Furthermore, I hypothesize that such cells are not compromising their physiological and social characteristics.

To test that *M. xanthus* can be labelled via Kdo-N_3-click chemistry-based reaction, I first sought to (i) synthesize Kdo-N_3 *in vitro* (in collaboration with the laboratory of Pr. Charles Gauthier). (ii) Uptake-and-incorporation of Kdo-N_3 into the *M. xanthus* OM was then tested via supplementation of liquid cultures with Kdo-N_3 followed by click chemistry-based fluorescence labelling of exposed -N_3 groups at the cell surface, (iii) as verified via single-cell fluorescence microscopy and in-gel fluorescence of extracted “clicked” LPS. Finally, (iv) phenotypic characterization of gliding motility, T4P-dependent motility, and fruiting body formation was performed for *M. xanthus* elaborating Kdo-N_3 in its LPS to test the effect of the incorporated synthetic sugar on the multicellular lifecycle of the bacterium.

3 MATERIALS AND METHODS

3.1 CHEMICAL SYNTHESIS OF KDO-N_3

Synthesis of Kdo-N_3 was carried out through a series of six-step chemical reactions, beginning with D-arabinose as a starting compound. Experimental details for each intermediate molecule generated are included in the respective Results sections. After each reaction, generated products were first analyzed by dissolving 1 mg in 1 mL of methanol, followed by spotting the product with 10 µL glass microcapilars at the bottom of a silica-covered thin-layer chromatography (TLC) plate. Samples were then resolved on TLC plates following a single run of solvent to the top of the plate in a glass tank. The staining agents used to develop the TLC plates were orcinol (1 mg/mL) in a $10\%_{aq.}$ solution of H_2SO_4 and/or Henessian's stain with a heat gun as a heating agent. Following TLC visualization, reaction products were purified by the laboratory of Prof. Charles Gauthier via flash chromatography and subjected to validation via ^{1}H and ^{13}C NMR when needed to verify the chemical structure of reaction intermediate (Ravicoularamin, 2019).

3.2 *MYXOCOCCUS XANTHUS* GROWTH CONDITIONS AND MEDIA

Myxospores of *M. xanthus* DZ2 **(Table 1)** were recovered from -80 ºC freezer stocks and streaked on CYE 1.5% agar plates **(Table 2)**. Once the plates were inoculated, they were sealed with Parafilm and incubated face-down at 32 ºC for 72 h in the dark. Pre-cultures were then set-up in an Erlenmeyer flask containing 12 mL of CYE liquid medium **(Table 2)** and *M. xanthus* cells recovered with a loop from incubated plates. Pre-cultures were incubated overnight at 32 ºC on a shaking incubator rotating at 220 rpm.

3.3 OUTER MEMBRANE LABELLING AND IMAGING

3.3.1 Kdo-N_3 incorporation

For a given strain, 1000 µL of CYE liquid medium was added to each of two glass tubes. The optical density at 600 nm (OD_{600}) was then read for the overnight pre-culture for each strain using a disposable cuvette (100 µL culture + 900 µL TPM buffer **[Table 2]** in cuvette, OD_{600} reading multiplied by 10 to obtain the true culture density). Based on the OD_{600} of the pre-culture, sufficient pre-culture volume was removed via micropipette and used to inoculate the 1000 µL duplicate volumes to an initial OD_{600} of 0.02. Tube #1 was set aside as the untreated

reference sample. To Tube #2, 25 µL of 200 mM Kdo-N_3 stock solution (dissolved in CYE liquid medium) was added, resulting in a 5 mM final concentration of Kdo-N_3 in Tube #2. Given the relatively low volume of the culture (i.e. 1 mL), the caps for Tubes #1 and #2 were both sealed with Parafilm to reduce evaporation of culture liquid, followed by incubation of both tubes (inclined in a tube rack) at 32 ºC in a shaking incubator (170 rpm) for 24 h. Following this incubation, to minimize wastage of culture volume, 1/10th OD_{600} readings of each subculture were taken (i.e. 100 µL culture + 900 µL TPM buffer) were read as before using a disposable cuvette and a spectrophotometer, with this value multiplied by 10 to reflect the true density of the culture. The remaining ~900 µL of culture volume in Tubes #1 and #2 was then meticulously split between experiments for (i) single-cell fluorescence microscopy, (ii) phenotype plate inoculation, and (iii) LPS extraction, as outlined below.

3.3.2 SPAAC-based fluorescence labelling of *M. xanthus* cells for single-cell analysis

To prepare cells for analysis via fluorescence microscopy, the specific culture volume to remove from Tube #1 (i.e. untreated cells) and Tube #2 (i.e. containing Kdo-N_3-grown cells) (see section **3.3.1**) was calculated so that, following sedimentation, resuspension of the cell pellet in 10 µL TPM buffer would yield an OD_{600} of 1.0. As such, from each tube, this calculated volume was removed twice, with each volume transferred to a separate 1.5 mL microfuge tube. Therefore, microfuge tubes with culture volume were designated for Sample #1A and 1B, as well as Sample #2A and 2B. For all four tubes, culture volumes were thus sedimented in a benchtop microfuge (6010 × *g*, 5 min) followed by aspiration via micropipette of the ensuing supernatants. Using a micropipette, each pellet was resuspended via aspiration and ejection in 10 µL of PBS buffer (wash 1), sedimented (6010 × *g*, 5 min) followed by supernatant removal, resuspended in 10 µL of PBS buffer (wash 2), and sedimented again (6010 × *g*, 5 min) followed by supernatant aspiration. Pellets for Samples #1A and 2A were then resuspended in 10 µL of PBS, whereas pellets for Samples #1B and 2B were resuspended in 10 µL of 30 µM DBCO-sulforhodamine **(Table 3)** solution (prepared in PBS). All four tubes were then placed in a microfuge tube rack, covered with aluminium foil, and incubated at 37 ºC (30 min) with shaking (170 rpm) to promote the SPAAC click reaction between -N_3 and DBCO. All tubes were then sedimented (6010 × *g*, 5 min), followed by supernatant aspiration and pellet resuspension in 10 µL of PBS buffer (wash 3). Tubes were again sedimented (6010 × *g*, 5 min), followed by supernatant aspiration and pellet resuspension in 10 µL of PBS buffer (wash 4), then sedimented one last time (6010 × *g*, 5 min). Finally, cells were resuspended in 10 µL of CYE

liquid medium to yield an OD_{600} of 1.0, prior to imaging on agar pads via fluorescence microscopy.

3.3.3 Fluorescence microscopy of SPAAC-labelled *M. xanthus* cells

For fluorescence microscopy, 1.5% agar pads were made by adding 0.15 g of low-melt agar to 10 mL of double distilled H_2O (ddH_2O), followed by heating in a microwave to dissolve the agar. Using a micropipette, molten agar was then added to a set of stacked glass microsope slides forming a channel in the middle, followed by covering of the filled channel with another microscope slide. Once solidified, this agar block was cut (using a scalpel blade) into square pads. For each final cell resuspension (see section **3.3.2**), 5 µL was spotted on a long glass coverslip and overlayed with a cut pad of agar. Imaging was carried out at 32 ºC on a Zeiss AxioObserver 7 fluorescence microscope, using the 40× objective with CY3 filter settings (suitable to detect fluorescence of sulforhodamine), and an acquisition time of 50 ms. Brightfield imaging for the same fields of view was carried out with the same objective, with DIA filter settings and an acquisition time of 10 ms. Movies were recorded for 30 min, with images captured at intervals of 30 s.

3.3.4 Analyses of *M. xanthus* motility and developmental phenotypes

To prepare cells for phenotypic analyses via stereoscopy, the specific culture volume to remove from Tube #1 (i.e. untreated cells) and Tube #2 (i.e. containing Kdo-N_3-grown cells) (see section **3.3.1**) was calculated so that, following sedimentation, resuspension of the cell pellet in 60 µL TPM buffer would yield an OD_{600} of 5.0. As such, from each tube, this calculated volume was removed twice, with each volume transferred to a separate 1.5 mL microfuge tube. Therefore, microfuge tubes with culture volume were designated for Sample #1A and 1B, as well as Sample #2A and 2B. For all four tubes, culture volumes were thus sedimented in a benchtop microfuge (6010 × *g*, 5 min) followed by aspiration via micropipette of the ensuing supernatants. Using a micropipette, each pellet was resuspended via aspiration and ejection in 60 µL of PBS buffer (wash 1), sedimented (6010 × *g*, 5 min) followed by supernatant removal, resuspended in 60 µL of PBS buffer (wash 2), and sedimented again (6010 × *g*, 5 min) followed by supernatant aspiration. Pellets for Samples #1A and 2A were then resuspended in 60 µL of PBS, whereas pellets for Samples #1B and 2B were resuspended in 60 µL of 30 µM DBCO-sulforhodamine **(Table 3)** solution (prepared in PBS). All four tubes were then placed in a microfuge tube rack, covered with aluminium foil, and incubated at 37 ºC (30 min) with shaking

(170 rpm) to promote the SPAAC click reaction between -N_3 and DBCO. All tubes were then sedimented (6010 × *g*, 5 min), followed by supernatant aspiration and pellet resuspension in 60 µL of PBS buffer (wash 3). Tubes were again sedimented (6010 × *g*, 5 min), followed by supernatant aspiration and pellet resuspension in 60 µL of PBS buffer (wash 4), then sedimented one last time (6010 × *g*, 5 min). Finally, cells were resuspended in 60 µL of TPM buffer to yield an OD_{600} of 5.0. In a biosafety hood, 5 µL of cell resuspension for each sample was spotted on (i) a square CYE 1.5% agar plate to probe gliding motility via swarm-edge flare formation, (ii) a square CYE 0.5% agar plate to study T4P-dependent motility and swarm expansion, and (iii) a square CF 1.5% agar plate to investigate fruiting body formation. Once inoculated cell volumes had dried down to the agar surface, all plates were sealed with Parafilm and incubated upside down at 32 ºC for either 24 h (for gliding flares), 48 h (for T4P-dependent swarm expansion), or 72 h (for fruiting body formation). At the end of the respective incubation period, swarms were imaging using an Olympus SZX16 fluorescence stereoscope.

3.3.5 Extraction of SPAAC-labelled LPS via the Hitchcock and Brown method

To prepare cells for LPS isolation via the Hitchcock and Brown (H&B) method (Hitchcock & Brown, 1983), the specific culture volume to remove from Tube #1 (i.e. untreated cells) and Tube #2 (i.e. containing Kdo-N_3-grown cells) (see section **3.3.1**) was calculated so that, following sedimentation, resuspension of the final cell pellet in 62.5 µL of H&B lysis buffer would yield an OD_{600} of 1.8. As such, from each tube, this calculated volume was removed twice, with each volume transferred to a separate 1.5 mL microfuge tube. Therefore, microfuge tubes with culture volume were designated for Sample #1A and 1B, as well as Sample #2A and 2B. For all four tubes, culture volumes were thus sedimented in a benchtop microfuge (6010 × *g*, 5 min) followed by aspiration via micropipette of the ensuing supernatants. Using a micropipette, each pellet was resuspended via aspiration and ejection in 62.5 µL of PBS buffer (wash 1), sedimented (6010 × *g*, 5 min) followed by supernatant removal, resuspended in 62.5 µL of PBS buffer (wash 2), and sedimented again (6010 × *g*, 5 min) followed by supernatant aspiration. Pellets for Samples #1A and 2A were then resuspended in 62.5 µL of PBS, whereas pellets for Samples #1B and 2B were resuspended in 62.5 µL of 30 µM DBCO-sulforhodamine **(Table 3)** solution (prepared in PBS). All four tubes were then placed in a microfuge tube rack, covered with aluminium foil, and incubated at 37 ºC (30 min) with shaking (170 rpm) to promote the SPAAC click reaction between -N_3 and DBCO. All tubes were then sedimented (6010 × *g*, 5 min), followed by supernatant aspiration and pellet resuspension in 62.5 µL of PBS buffer (wash 3). Tubes were again sedimented (6010 × *g*, 5 min), followed by supernatant aspiration and

pellet resuspension in 62.5 µL of PBS buffer (wash 4), then sedimented one last time (6010 × *g*, 5 min). Finally, cells were resuspended in 62.5 µL of H&B lysis buffer lacking reducing agent (as the presence of reducing agent would break the -N_3–DBCO bond) to yield an OD_{600} of 1.8. All four tubes were heated at 100 ºC in a boiling water bath for 30 min. Once cooled, 2 µL of a 20 mg/mL Proteinase K solution was added to each tube. Samples were incubated overnight at 55 ºC in a stationary incubator to non-specifically digest all protein in the cell lysates, leaving intact the various lipid species including LPS from the OM.

3.3.6 In-gel fluorescence analysis of SPAAC-labelled LPS

Firstly, 10% polyacrylamide resolving gels (1 mm thickness) were first cast, followed by 5% polyacrylamide stacking gels (1 mm thickness, 10 wells). To analyze the LPS isolated via the H&B method, 25 µL of each sample were loaded in a well, followed by electrophoresis in SDS-PAGE running buffer. Samples were focused by running through the stacking gel for 25-30 min at 80 V; samples were subsequently resolved via running through the resolving gel for 45 min at 120 V. Throughout the sample migration period, gel tanks were covered with aluminum foil to keep them in the dark and avoid photobleaching of resolved fluorescent bands. Post-electrophoresis, resolved gels were scanned on a Typhoon fluorescence scanner (GE-Typhoon FLA 9000) to detect in-gel fluorescence of the SPAAC-labelled LPS bands, using the 532 nm laser for excitation of the sulforhodamine fluorophore and the LPR emission filter to select for the fluorescence signal.

Table 1. List of *M. xanthus* strains.

Strains	Features	Reference
DZ2	Wild Type	(Campos & Zusman, 1975)

Table 2. Growth media and buffer compositions

Media / Solution	Components
CYE medium	• 10 mM morpholinepropanesulfonic acid (MOPS), pH 7.6 • 10 g/L Casitone • 5 g/L yeast extract • 8 mM $MgSO_4$
CF medium	• 10 mM MOPS, pH 7.6 • 1 mM KH_2PO_4 • 8 mM $MgSO_4$ • 0.02% $(NH_4)_2SO_4$ • 0.2% citrate • 0.2% pyruvate • 150 mg/L Casitone
TPM	• 10 mM Tris-HCl pH 7.6 • 1 mM KH_2PO_4 • 8 mM $MgSO_4$
Hitchcock and Brown lysis buffer	• 2% SDS • 4% β-mercaptoetanol • 10% glycerol • 1M Tris-HCl pH 6.8 • 4% β-mercaptoetanol
Stacking Gel (SDS-PAGE)	• 0.68 mL H_2O • 0.17 mL 30% acrylamide mix • 0.13 mL 1.5 M Tris (pH 8.8) • 0.01 mL 10% SDS • 0.01 mL 10% ammonium persulfate • 0.001 TEMED

Resolving Gel (SDS-PAGE)	• 1.6 mL H_2O • 1.7 mL 30% acrylamide mix • 1.3 mL 1.5 M Tris (pH 8.8) • 0.05 mL 10% SDS • 0.05 mL 10% ammonium persulfate • 0.002 TEMED
Tris/Glycine Buffer (10X)	• 25 mM Tris • 192 mM glycine • 0.1% SDS
PBS (1X)	• 137 mM NaCl • 2.7 mM KCl • 10 mM Na_2HPO_4 • 1.8 mM KH_2PO_4

Table 3. Click chemistry components.

Component	**Source**
Kdo-N_3	Synthesized in collaboration by laboratories of Profs. Charles Gauthier and Salim Timo Islam
DBCO-Sulforhodamine	Click Chemistry Tools *(CLK-A132-5)*

4 RESULTS

4.1 KDO-N_3 SYNTHESIS

Given the success of OM functionalization with Kdo-N_3 **(Figs. 12B and 13)**, and to continue with our experiments, we first optimized synthesis of our own Kdo-N_3 **(Fig. 11)** as it is commercially expensive ($1500 for 10 mg).

4.1.1 Synthesis of 1,2,3-tri-O-acetyl-5-O-trityl-D-arabinofuranose

D-Arabinose **molecule 1** (10.0 g, 67 mmol, 1 eqv) was stirred in refluxing pyridine (350 mL) until it dissolved, the solution was then allowed to cool to 25 ºC. Trityl chloride (18.6 g, 67 mmol, 1 eqv) was added in one portion and the reaction stirred under an argon atmosphere for 48 h while ensuring the temperature did not exceed 30 ºC. The reaction was quenched with methanol (25 mL) and the solvent was subsequently removed by evaporation in vacuo (**Fig. 14)**

A)

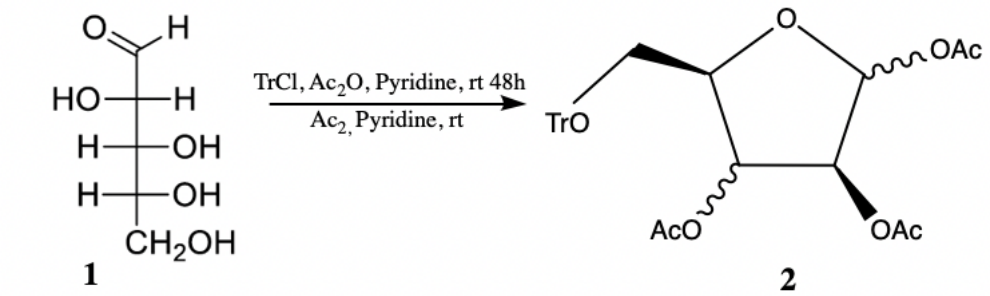

B)

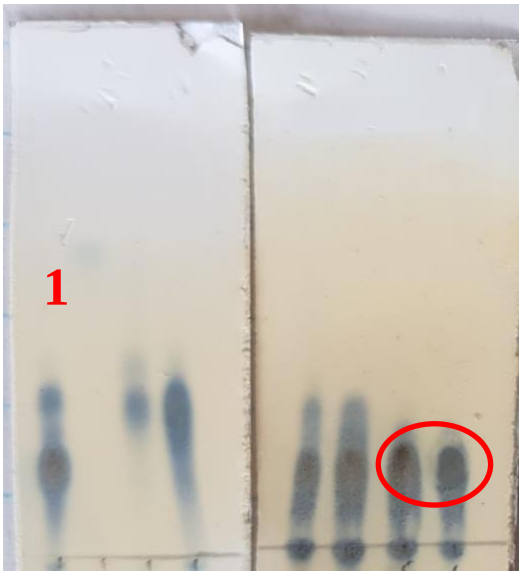

Figure 14. Synthesis of 1,2,3-tri-O-acetyl-5-O-trityl-D-arabinofuranose

(A) Chemical reaction carried out. **(B)** Initial verification of molecule 2 production via TLC of the elution fractions of interest obtained from the purification system. Lane 1 in TLC left plate corresponds to the profile of all the fractions that are expected to be separated.

4.1.2 Synthesis of 1,2,3-tri-O-acetyl-D-arabinofuranose

Trityl ether **molecule 2** (10 g, 19.29 mmol) was stirred in 80% aqueous AcOH (100 mL) at 100 ºC for 25 min and cooled immediately in an ice-bath. The trityl alcohol by-product that crystallised was filtered off, the filtrate treated with brine (100 mL) and extracted with dichloromethane DCM (3 × 40 mL). The organic layers were combined, washed with sat $NaHCO_3$ (aq), dried over $MgSO_4$ and concentrated by evaporation in vacuo **(Fig. 15)**.

A)

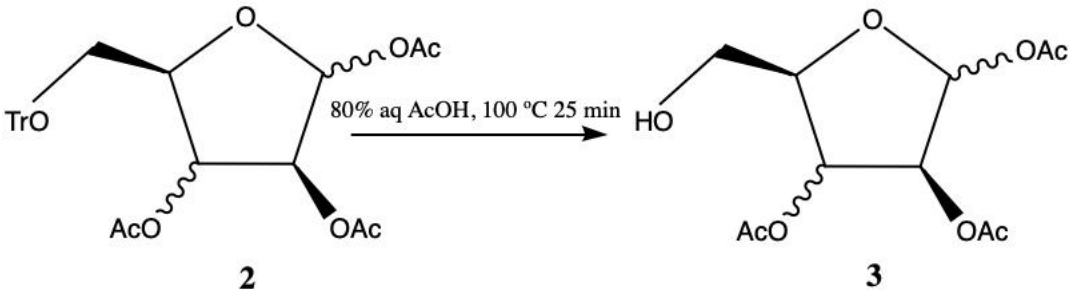

B)

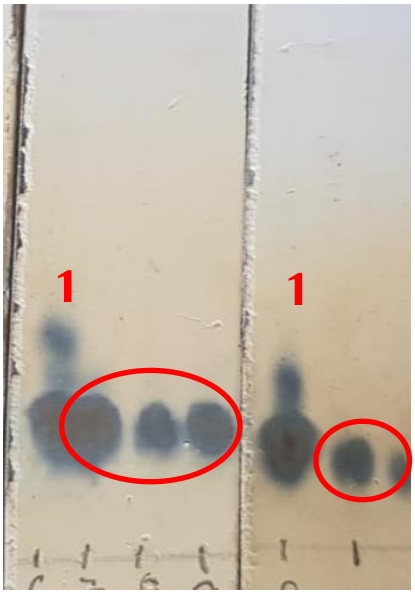

Figure 15. Synthesis of 1,2,3-tri-O-acetyl-D-arabinofuranose

(A) Chemical reaction carried out. **(B)** Initial verification of molecule 3 production via TLC of the elution fractions of interest obtained from the purification system. Lane 1 in both TLC plates (Left and Right) corresponds to the profile of all the fractions that are expected to be separated.

4.1.3 Synthesis of 1,2,3-tri-O-acetyl-5-O-tosyl-D-arabinofuranose

The primary alcohol **molecule 3** (1.83 g, 6.6 mmol, 1 eqv) was dissolved in dry DCM (40 mL) and pyridine (5 mL). Tosyl chloride (1.9 g, 9.9 mmol 1.5 eqv) was added slowly before leaving the reaction to stir at room temperature for 48 h under an atmosphere of argon. The reaction mixture was washed with water and the aqueous layer was further extracted with DCM (3 × 20 mL). The combined organic layers were washed with 1 M HCl (40 mL), sat $NaHCO_3$ (aq), and brine (40 mL) before being dried over $MgSO_4$ and concentrated by evaporation in vacuo **(Fig. 16)**.

A)

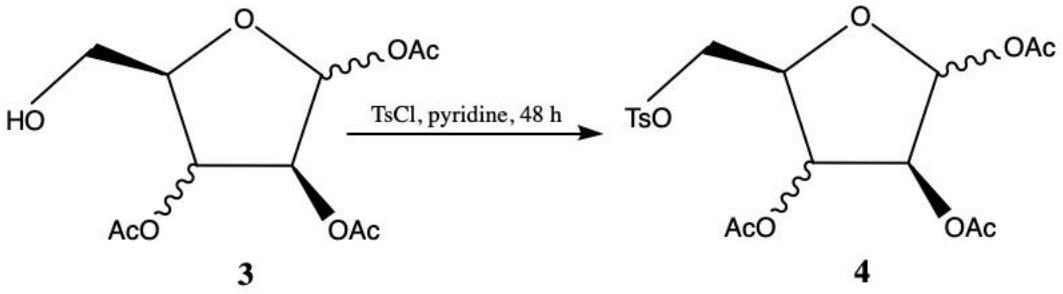

3 4

B)

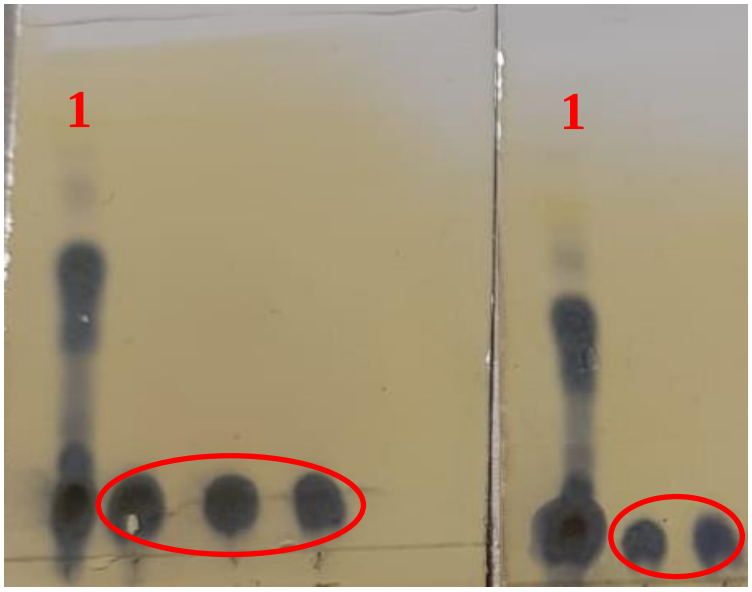

Figure 16. Synthesis of 1,2,3-tri-O-acetyl-5-O-tosyl-D-arabinofuranose

(A) Chemical reaction carried out. **(B)** Initial verification of molecule 4 production via TLC of the elution fractions of interest obtained from the purification system. Lane 1 in both TLC plates (Left and Right) corresponds to the profile of all the fractions that are expected to be separated.

4.1.4 Synthesis of 1,2,3-tri-O-acetyl-5-azido-5-deoxy-D-arabinofuranose

Tosylate **molecule 4** (1.1 g, 2.6 mmol) and sodium azide (0.7 g, 10 mmol, 3 eqv) were heated to 80 ºC in DMSO (15 mL) under an atmosphere of argon for 24 h. On cooling, the reaction mixture was diluted with DCM (40 mL) and washed with water (200 mL) before drying the organic layer over $MgSO_4$ and concentrated in vacuo **(Fig. 17)**.

A)

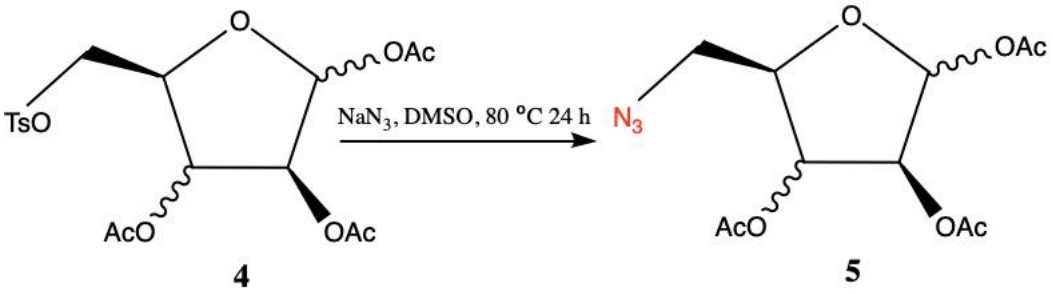

B)

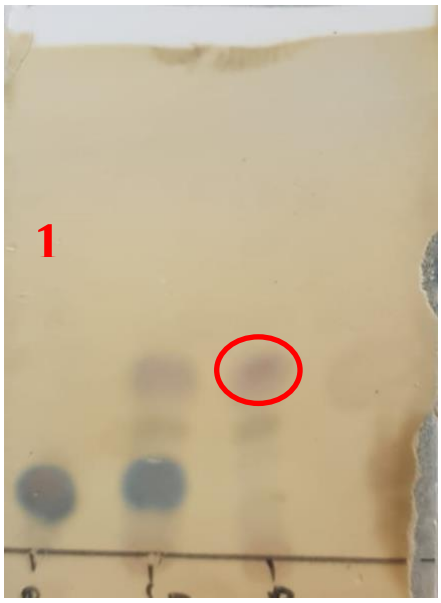

Figure 17. Synthesis of 1,2,3-Tri-O-acetyl-5-azido-5-deoxy-D-arabinofuranose

(A) Chemical reaction carried out. **(B)** Initial verification of molecule 5 production via TLC of the elution fractions of interest obtained from the purification system. Lane 1 in TLC plate corresponds to the profile of all the fractions that are expected to be separated.

4.1.5 Synthesis of 5-azido-5-deoxy-D-arabinofuranose

Triacetate **molecule 5** (480 mg, 1.60 mmol) was dissolved in dry methanol (10 mL). Sodium methoxide (9 mg, 0.16 mmol) was added and the reaction mixture was stirred at room temperature under an argon atmosphere. Dowex ion exchange resin was added until pH paper indicated the reaction mixture was pH neutral. The solid material was filtered off and the filtrate concentrated in vacuo **(Fig. 18)**.

A)

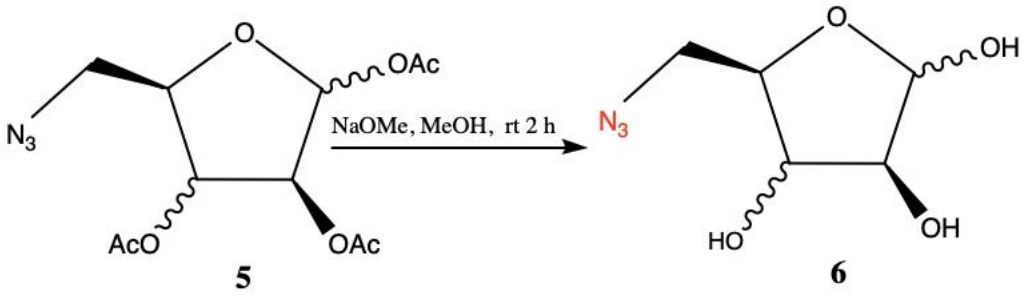

B)

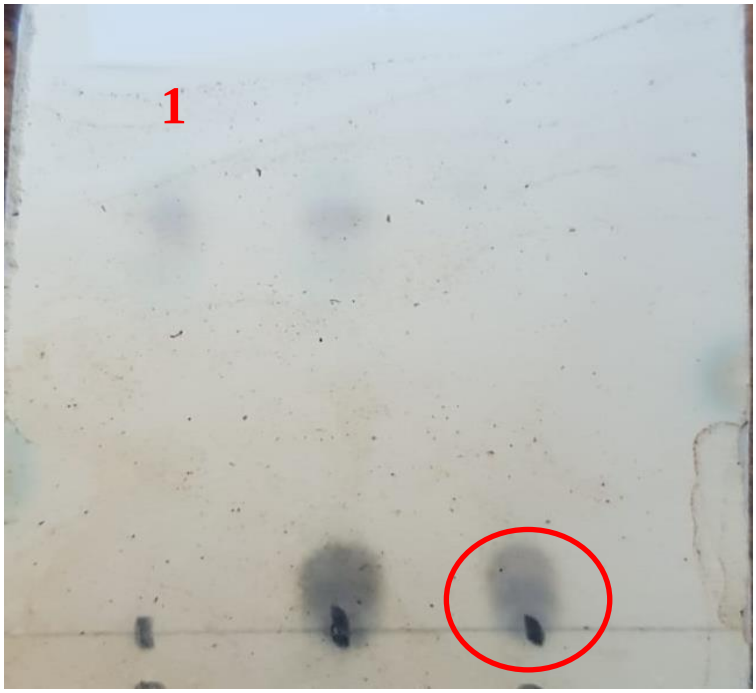

Figure 18. Synthesis of 5-Azido-5-deoxy-D-arabinofuranose

(A) Chemical reaction carried out. **(B)** Initial verification of molecule 6 production via TLC of the elution fractions of interest obtained from the purification system. Lane 1 in TLC plate corresponds to the profile of all the fractions that are expected to be separated.

4.1.6 Synthesis of ammonium 8-azido-3,8-dideoxy-D-manno-oct-2-ulopyranosylonate (Kdo-N_3)

Arabinose-N_3 **molecule 6** (350 mg, 2.0 mmol, 1.0 equiv) was dissolved in distilled H_2O (6.0 mL) containing Na_2CO_3 (526 mg, 4.9 mmol, 2.5 equiv). Crystals of oxaloacetic acid (317 mg, 2.4 mmol, 1.2 equiv) were added in small portions over five min. After adding few drops of 10.0 N aq. NaOH solution until the pH of the mixture was increased to 11, the reaction mixture was stirred for 2 h. pH was further brought down to 5.0 using AcOH, followed by the addition of $NiCl_2$*$6H_2O$ (0.01 equiv) and stirred at 50 ºC for 1 h. After cooling the mixture, anion exchange resin column CG-400 (HCO_3-) was used. It was first eluted with H_2O to remove the excess of arabinose-N_3, followed by aq. NH_4HCO_3 (0.05–0.30 N). The fractions were pooled and lyophilized to obtain desired Kdo-N_3 as white amorphous solid **(Fig. 19)**.

A)

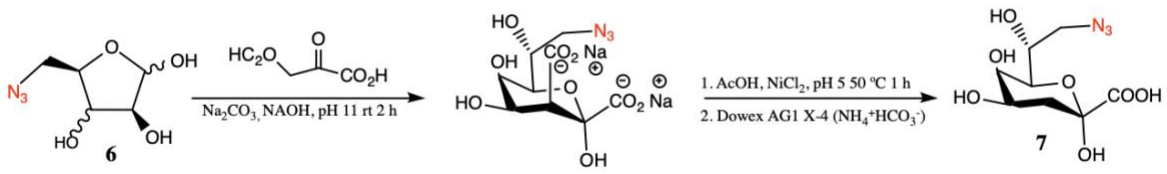

B)

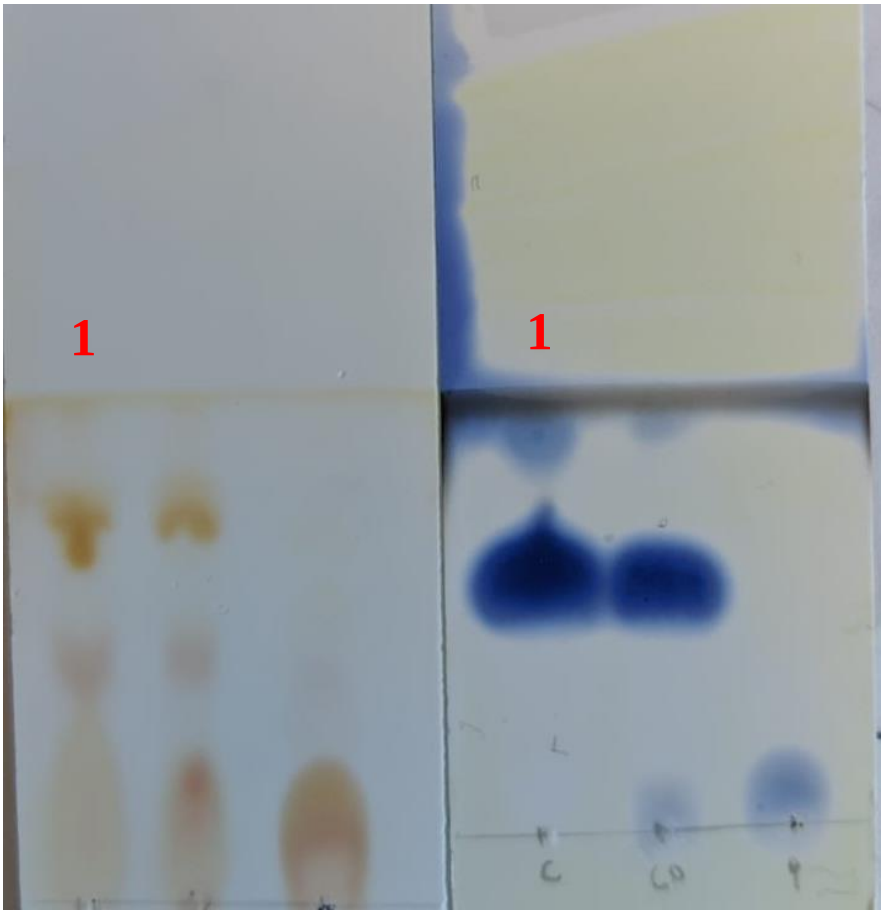

Figure 19. Synthesis of Ammonium 8-Azido-3,8-dideoxy-D-manno-oct-2-ulopyranosylonate (Kdo-N_3)

(A) Chemical reaction carried out. **(B)** Initial verification of molecule 7 production via TLC of the elution fractions of interest obtained from the purification system. Left and Right TLC plates correspond to the same reaction, additional Hanessian's staining was performed as a second control for the reaction *(Right TLC plate)*. Lane 1 in TLC plates (Right and Left) corresponds to the profile of all the fractions that are expected to be separated.

4.2 CLICK CHEMISTRY TARGETING THE *M. XANTHUS* CELL SURFACE

For testing click-mediated labelling of the *M. xanthus* OM, a protocol had to be implemented as such labelling of the *M. xanthus* OM had never been attempted before. The protocol used for OM labeling worked as expected, based on Kdo-N_3 incorporated into the LPS by outcompeting native Kdo **(Fig. 21A)**, followed by click-mediated SPAAC labelling of the *M. xanthus* OM with DBCO-dye **(Fig. 21B)**.

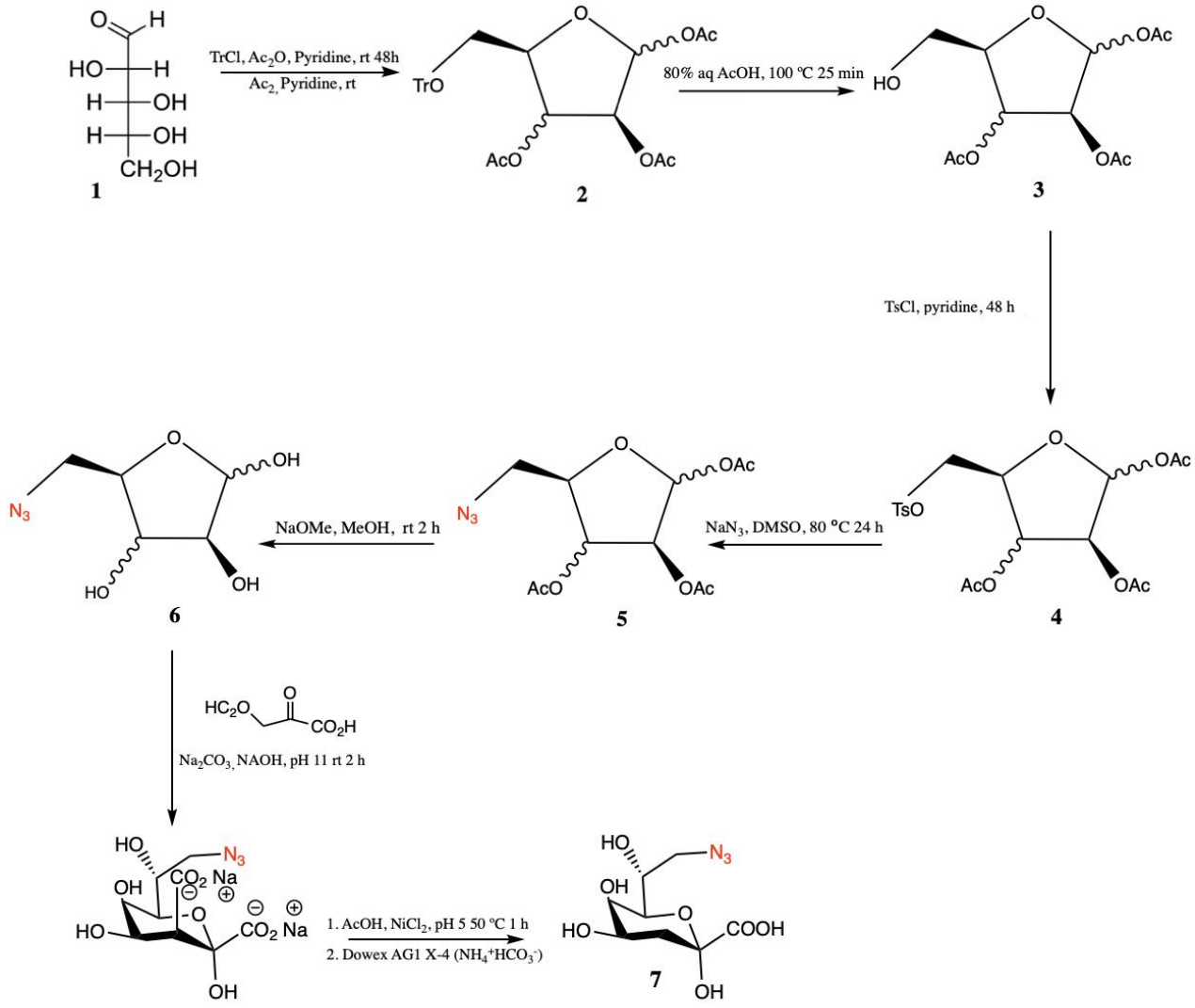

Figure 20. Complete synthesis pathway for the production of Kdo-N_3

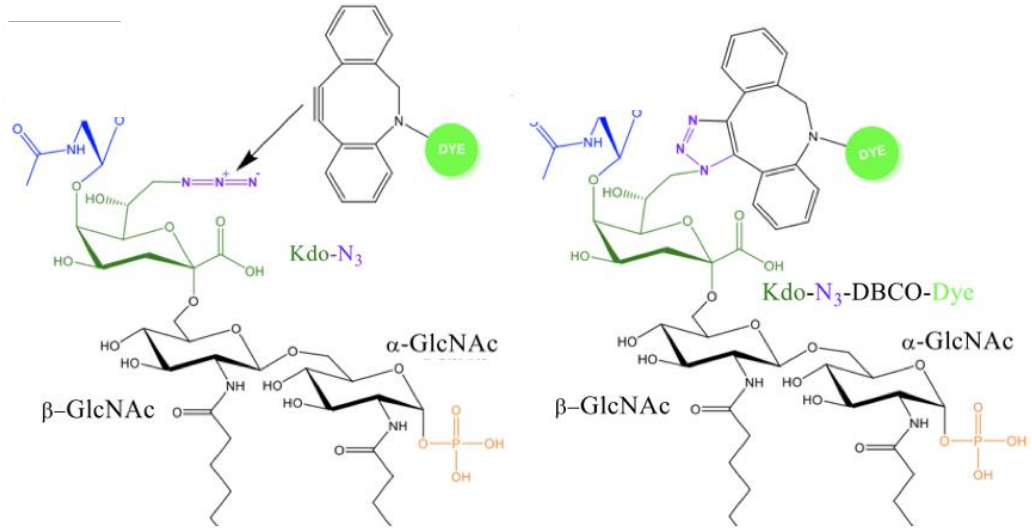

Figure 21. Partial proposed structure of *M. xanthus* LPS during SPAAC reaction

Left panel: Kdo-N_3 synthetic sugar incorporated into the core OS and the attacking group of DBCO conjugated to a generic fluorescent dye. *Right panel* Structure of the core OS following SPAAC labelling of the -N_3 motif of Kdo-N_3. (Image courtesy of S.T. Islam, unpublished, used with permission). Refer to Fig. 7B for a full depiction of the *M. xanthus* LPS molecule.

4.3 OUTER MEMBRANE LABELLING AND IMAGING

4.3.1 Single-cell fluorescence imaging

Single *M. xanthus* cells, grown in the presence of Kdo-N_3 and clicked with DBCO-sulforhodamine were successfully visualized via fluorescence microscopy, whereas cells treated with the labelling reagent alone were not fluorescent **(Fig. 22)**. This suggests that Kdo-N_3 was successfully internalized by the cells and incorporated into nascent LPS, after transport to the cell surface and insertion into the outer leaflet of the OM, where the exposed -N_3 group could be successfully clicked with DBCO-sulforhodamine **(Fig. 21)**.

4.3.2 *M. xanthus* phenotypic analysis

After testing single-cell OM labelling with click chemistry methodology, a second experiment was performed in order to analyze if the incorporation of Kdo-N_3 would affect the community-scale motility and developmental physiology of *M. xanthus*. On hard CYE 1.5% agar plates, gliding motility-dependent swarm-edge flares were observed regardless of treatment, suggesting that Kdo-N_3 incorporation as well as click labelling does not impact gliding motility **(Fig. 23)**. T4P-dependent group motility and swarm expansion was similarly not affected, irrespective of treatment **(Fig. 23)**. Finally, on nutrient-poor CF 1.5% agar plates, fruiting body structures could still form in the presence or absence of Kdo-N_3 **(Fig. 23)**. Therefore, *M. xanthus* elaborating LPS containing Kdo-N_3 does not appear to be compromised for typical motility and developmental outcomes.

4.4 *MYXOCOCCUS XANTHUS* LPS EXTRACTION

Finally, a third test was performed in order to confirm the incorporation of Kdo-N_3 into the LPS and therefore the correct click-chemistry labelling. LPS extraction was performed by Hitchcock and Brown preparation (Hitchcock & Brown, 1983) after click labelling of *M. xanthus* cells. After the extraction, samples were run on an SDS-PAGE gel and imaged on a Typhoon scanner in order to detect LPS signal in the expected lane of the gel. For the SDS-PAGE gel WT control and WT with the elements of click-chemistry labelling were loaded side by side in order to observe the difference of signal after the Typhoon scan **(Fig. 24).**

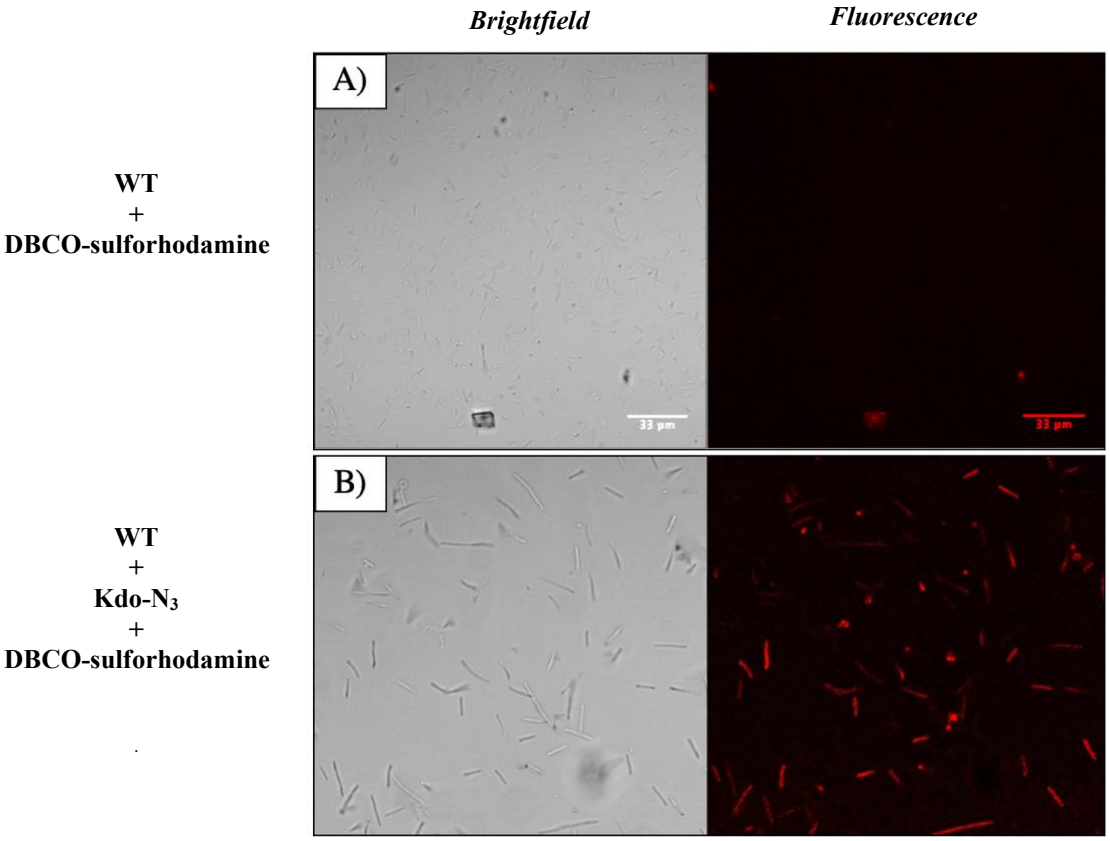

Figure 22. Fluorescence microscopy following SPAAC of *M. xanthus* cells grown in the presence of Kdo-N_3

(A) Brightfield and fluorescence micrographs of *M. xanthus* WT cells grown in the absence of Kdo-N_3, but still treated for SPAAC labelling with DBCO-sulforhodamine. **(B)** Brightfield and fluorescence micrographs of *M. xanthus* WT cells grown in the presence of Kdo-N_3 and treated for SPAAC labelling with DBCO-sulforhodamine.

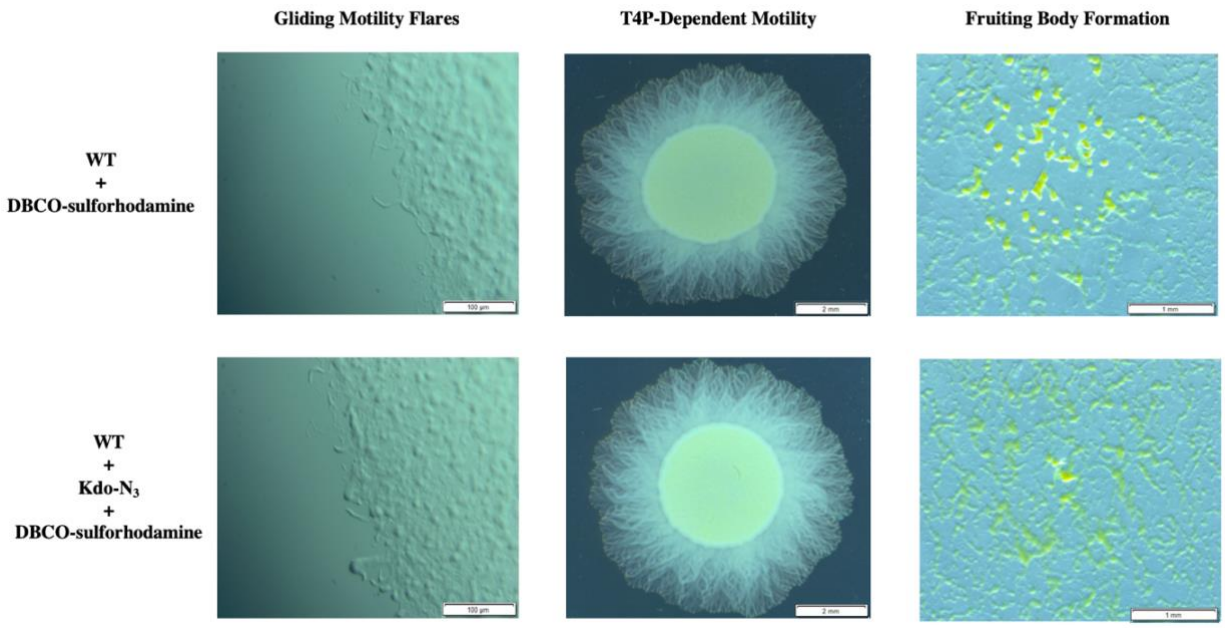

Figure 23. Motility and developmental phenotypes of *M. xanthus* with incorporated Kdo-N_3

The first row shows untreated WT cells as a reference for typical formation of gliding motility-dependent swarm-edge flares (scale bar = 100 µm) on hard CYE 1.5% agar, T4P-dependent swarm expansion (scale bar = 2 mm) on soft CYE 0.5% agar, and fruiting body formation (scale bar = 1 mm) on hard CF 1.5% minimal agar. The second row depicts WT cells, grown in the presence of Kdo-N_3, and treated with DBCO-sulforhodamine.

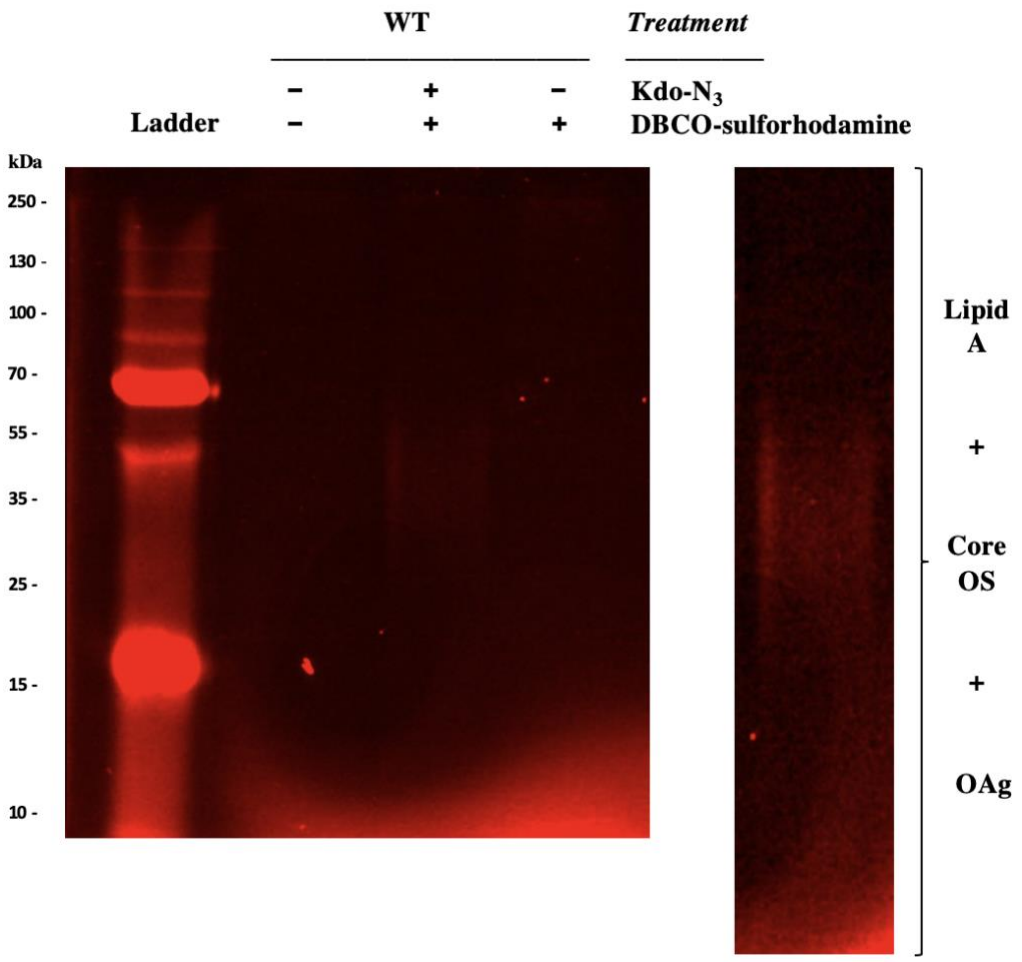

Figure 24. In-gel fluorescence of SDS-PAGE-resolved DBCO-sulforhodamine-labelled *M. xanthus* LPS

In the 1st lane, a protein ladder was run simply to indicate migration of samples through the gel. The 2nd, 3rd, and 4th lanes contain LPS extracted from WT that had undergone various incubations and treatments. *Right side:* The 3rd lane has been magnified to better show the resolution of fluorescent LPS bands all containing Lipid A, core OS, and a preferred modal range of different lengths of OAg.

5 DISCUSSION

5.1 CLICK-CHEMISTRY OM LABELLING AND IMAGING IN *MYXOCOCCUS XANTHUS*

Click chemistry is an emerging technology with high potential, and it is only recently that it has been adapted for cell-labelling projects, with its main advantages being its high specificity, quick reaction time, and potential for use on living cells without compromising viability. *E. coli* has been the most recurrent model while implementing click chemistry technology. The Dukan lab has reported the succesfull labeling of *E. coli* while using copper-catalized click reactions (Dumont *et al., 2012)*. For my project, the use of a Gram-negative model and click chemistry reaction that can allow the cell-labelling while eliminate a toxic catalyst, was highly important and significantly different as previous methodologies reported. During the development of this project the methodology for labeling *M. xanthus* OM was realized by click chemistry, in which Kdo-N_3 was incorporated into *M. xanthus* LPS in order to perform a click reaction between the azide (N_3) and DBCO-sulfurhodamine dye, after this reaction, fluorescent-cell microscopy was performed, to analyze the results and the efficiency and the possible social and physiological effects that *M. xanthus* might present by using this methodology. During the selection of methodology for the OM labeling of *M. xanthus,* several analyses of the possible effects that could lead this technology were made referring to the possibility of presenting any impairment of *M. xanthus* behaviour, and/or cell modifications.

One of the main reasons for click chemistry selection, was the suitability of perfoming a Cu-free click-reaction (SPAAC) in which there is no requirement for a copper catalyst (Bertozzi *et al.*, 2004). This allowed me to eliminate one highly toxic factor for cells that could affect the social and physiological characteristics of *M. xanthus.* As expected there were no appreciable changes in gliding motility, T4P-dependent motility, or fruiting body formation, between the samples that were tested, indicating a physiological acceptance of the synthetized Kdo-N_3 by the bacterium. For fluorescent labelling, I found similar results to those reported from the Dukan lab; while using this methodology in *E.coli* K12 (Dumont *et al.*, 2012) the Dukan lab did not report any altered physiology.

Moroever, the protocols implemented in this project are establishing how to work with *M. xanthus* cells for click-chemistry reactions, labelling of Kdo-N_3 with dyes, physiological assays (Phenotype analysis and Flouresence microscopy) and *in vitro* analysis via in-gel fluorescence. These are methods have not been reported before for use in *M. xanthus*, thus opening new doors and questions for *M. xanthus* research.

5.2 KDO-N_3 CHEMICAL SYNTHESIS AND PATHWAY EFFICIENCY AND FUTURE

8-Azido-3,8-dideoxy-D-manno-octulosonic acid (Kdo-N_3) is an analogue of the natural 3-deoxy-D-manno-octulosonic acid (Kdo) that contains a small modification, specifically an azido moiety. This synthetic Kdo-N_3 sugar molecule can be taken up by Gram-negative cells, and incorporated into glycans normally containing Kdo, during active glycan biosynthesis. Detection of the -N_3 group utilizes the chemoselective ligation or "click" reaction between an azide and an alkyne or cyclooctyne (Nilsson *et al.*, 2017).

For my MSc research, the synthesis of Kdo-N_3 was first realized so as to generate sufficient product for use in downstream experiments. The synthesis of this molecule can be considered "efficient" in terms of time and money invested. The complete synthesis had a duration of approximately 2 months, during which time the synthesis efficiency of the intermediate molecules of the chemical pathway was variant. Despite the synthesis pathway and functionality of the Kdo-N_3 molecule previously published (Dumont *et al.*, 2012), difficulties in reproducing the protocol led us to modify the published scheme in order to find the optimal synthesis pathway, the modification were mainly addressed in the duration and catalysts for the reactions, since in our particular case some of the reactions were not able to be fully achieved with the information that was reported in the chemical pathway mentioned before.

It can be said that one of the limitants for the project was Kdo-N_3, since the current market price of Kdo-N_3 is 1500 $ for 10 mg of sample. The price could bring an interesting economical debate for the price of this compound and if it is worth to invest in this technology and reactants. Given that in this project we were able to succesfully synthetize the molecule, it also resulted in an understanding of the price by analyzing the total synthesis duration that was invested for achieving this part of the project. We were able to synthetize 1 g of Kdo-N_3 which has a market value of 150,000 $, opening the possibility of investing part of this budget in more variables for click-chemistry reagents.

There are still few reported synthetic pathways in order to succesfully prepare Kdo-N_3, leaving room to the development of more efficient and straightforward procedures. In the years to come, new chemical pathways for synthetizing Kdo-N_3 and performing click chemistry reactions for cell labeling are expected to emerge since the technology is new and has gained interest in research.

6 PERSPECTIVES AND CONCLUSION

The technology used (click chemistry) and the protocols that were used for cell-labeling *in vivo* for the realization of this project, have constructed a solid base for the development of new projects and investigations that can be highly enriched and supported by this technology across a variety of experiments. Additional experimental data will further increase the robustness of the data I have presented in this MSc thesis, particularly with respect to single-cell effects of Kdo-N_3 incorporation. Parameters such as single-cell gliding speeds and reversal frequencies have yet to be examined to determine the potential impact of LPS labelling on cell–substratum coupling.

There are two projects that can be immediately pursued with this incredible technique. The first involves the examination of “active” vs. “passive” production of OMTs by *M. xanthus* over time. The LPS of *M. xanthus* contains only one Kdo sugar (modified with phosphoethanolamine [*P*EtN]) in the core OS, and branched Lipid A acyl chains. The methodology of metabolic labeling of cell-surface LPS can be used to demonstrate the hypothesis that *OMTs are not simply an outgrowth of cell shortening during senescence*. OMTs generated by fluorescently-“clicked” cells could be imaged over time via fluorescence microscopy and the obtained data can be analyzed using imaging software such as ImageJ which has all the tools necessary for single-cell behavior analysis.

The second aim that could be pursued with click chemistry methodology is identifying and characterizing proteins responsible for OM extrusion. As OMTs are generated at the poles (Ducret *et al.* 2013), any associated machinery should be similarly localized; thus, after induction of polar OMV production (Kahnt *et al.*, 2010) (and differential centrifugation to isolate the OMVs) in cells elaborating Kdo-N_3, can be lysated by a mechanical method. Once again benefitting from click chemistry, total OM material can be selectively isolated via covalent LPS binding to DBCO-linked magnetic beads, followed by magnetized bead removal from mixture. If developed, this will represent a revolutionary method for bacterial OM isolation, which usually takes 2 days of processing in a normal sucrose gradient centrifugation.

This project will help to elucidate the capacity of bacteria to maintain synergistic connections in heterogeneous environments through remodelling of their cell surfaces. The identification of OM extrusion as an active bacterial process, as well as any specific cellular factors contributing to the phenomenon, will enable the development of novel therapeutic agents targeted towards specific proteins and/or molecules responsible for the generation of these OM structures that are important for surface colonization and long-term persistence. For instance,

inhibiting OMV release during acute infections, or OMT formation in chronic infections, could serve to directly ameliorate negative disease outcomes. The OMV/OMT extrusion can also provide benefits for the wider bacterial community during infections, through the transfer of resistance or virulence factors. Thus, given the OMV/T production may affect the activities of antibacterial agents, and most importantly their production should be considered when administering antibacterial treatments (Mozaheb & Mingeot-Leclercq, 2020).

In conclusion, during the duration of this research, the hypothesis of this project was pursued and questioned with the click chemistry methodology development, fluorescence single-cell imaging and the physiological behavior analysis. This field of research (click labelling) is an emerging methodology that had never before been applied to *M. xanthus*; in the near future several projects will further elucidate this new field of research for this bacterium.

Finally, the data obtained in this project will have a positive impact on this emerging field of research. More importantly, it will eventually be possible to apply this knowledge towards developing microbe-centric therapies and therapeutics to target and disrupt the systems responsible for bacterial surface remodeling. By minimizing the ability of bacteria to colonize and persist in biological settings, health outcomes for patients with both acute and chronic infections will be improved.

7 BIBLIOGRAPHY

Atwal S, Giengkam S, VanNieuwenhze M,Salje J (2016) Live imaging of the genetically intractable obligate intracellular bacteria Orientia tsutsugamushi using a panel of fluorescent dyes. *Journal of microbiological methods* 130:169-176.

Bagheri M, Keller S,Dathe M (2011) Interaction of W-Substituted Analogs of Cyclo-RRRWFW with Bacterial Lipopolysaccharides: the Role of the Aromatic Cluster in Antimicrobial Activity. *Antimicrobial agents and chemotherapy* 55:788-797.

Bertani B & Ruiz N (2018) Function and Biogenesis of Lipopolysaccharides. *EcoSal Plus* 8(1).

Bertozzi CR, Agard NJ,Prescher JA (2004) A Strain-Promoted [3 + 2] Azide−Alkyne Cycloaddition for Covalent Modification of Biomolecules in Living Systems. *Journal of the American Chemical Society* 126(46):15046-15047.

Campos JM & Zusman DR (1975) Regulation of development in Myxococcus xanthus: effect of 3':5'-cyclic AMP, ADP, and nutrition. *Proc Natl Acad Sci U S A* 72(2):518-522.

Cao P & Wall D (2017) Self-identity reprogrammed by a single residue switch in a cell surface receptor of a social bacterium. *Proceedings of the National Academy of Sciences* 114(14):3732-3737.

Driessen AJ & Nouwen N (2008) Protein translocation across the bacterial cytoplasmic membrane. *Annu Rev Biochem* 77:643-667.

Ducret A, Fleuchot B, Bergam P,Mignot T (2013) Direct live imaging of cell-cell protein transfer by transient outer membrane fusion in Myxococcus xanthus. *Elife* 2:e00868.

Ducret A, Valignat M-P, Mouhamar F, Mignot T,Theodoly O (2012) Wet-surface–enhanced ellipsometric contrast microscopy identifies slime as a major adhesion factor during bacterial surface motility. *Proceedings of the National Academy of Sciences* 109(25):10036-10041.

Dumont A, Malleron A, Awwad M, Dukan S,Vauzeilles B (2012) Click-Mediated Labeling of Bacterial Membranes through Metabolic Modification of the Lipopolysaccharide Inner Core. *Angewandte Chemie International Edition* 51(13):3143-3146.

Dumont M, Lehner A, Vauzeilles B, Malassis J, Marchant A, Smyth K, Linclau B, Baron A, Mas Pons J, Anderson CT, Schapman D, Galas L, Mollet J-C,Lerouge P (2016) Plant cell wall imaging by metabolic click-mediated labelling of rhamnogalacturonan II using azido 3-deoxy-d-manno-oct-2-ulosonic acid. *The Plant Journal* 85(3):437-447.

Fugier E, Dumont A, Malleron A, Poquet E, Mas Pons J, Baron A, Vauzeilles B,Dukan S (2015) Rapid and Specific Enrichment of Culturable Gram Negative Bacteria Using Non-Lethal Copper-Free Click Chemistry Coupled with Magnetic Beads Separation. *PLoS One* 10(6):e0127700.

Gröst C & Berg T (2015) PYRROC: the first functionalized cycloalkyne that facilitates isomer-free generation of organic molecules by SPAAC. *Organic & Biomolecular Chemistry* 13(13):3866-3870.

Haurat MF, Elhenawy W,Feldman MF (2015) Prokaryotic membrane vesicles: new insights on biogenesis and biological roles. *Biol Chem* 396(2):95-109.

Hein CD, Liu XM,Wang D (2008) Click chemistry, a powerful tool for pharmaceutical sciences. *Pharm Res* 25(10):2216-2230.

Hein JE, Tripp JC, Krasnova LB, Sharpless KB,Fokin VV (2009) Copper(I)-catalyzed cycloaddition of organic azides and 1-iodoalkynes. *Angewandte Chemie (International ed. in English)* 48(43):8018-8021.

Himo F, Lovell T, Hilgraf R, Rostovtsev VV, Noodleman L, Sharpless KB,Fokin VV (2005) Copper(I)-Catalyzed Synthesis of Azoles. DFT Study Predicts Unprecedented Reactivity and Intermediates. *Journal of the American Chemical Society* 127(1):210-216.

Hitchcock PJ & Brown TM (1983) Morphological heterogeneity among Salmonella lipopolysaccharide chemotypes in silver-stained polyacrylamide gels. *J Bacteriol* 154(1):269-277.
Islam S & Lam J (2013) Topological mapping methods for α-helical bacterial membrane proteins – an update and a guide. *MicrobiologyOpen* 2:350-364.
Jain S & Darveau RP (2010) Contribution of Porphyromonas gingivalis lipopolysaccharide to periodontitis. *Periodontol 2000* 54(1):53-70.
Joo SH (2015) Lipid A as a Drug Target and Therapeutic Molecule. *Biomolecules & therapeutics* 23:510-516.
Kahnt J, Aguiluz K, Koch J, Treuner-Lange A, Konovalova A, Huntley S, Hoppert M, Søgaard-Andersen L,Hedderich R (2010) Profiling the outer membrane proteome during growth and development of the social bacterium Myxococcus xanthus by selective biotinylation and analyses of outer membrane vesicles. *J Proteome Res* 9(10):5197-5208.
Kang K, Park J,Kim E (2016) Tetrazine ligation for chemical proteomics. *Proteome Sci* 15:15.
Kolb HC, Finn MG,Sharpless KB (2001) Click Chemistry: Diverse Chemical Function from a Few Good Reactions. *Angewandte Chemie International Edition* 40(11):2004-2021.
Lindberg AA, Weintraub A, Zähringer U,Rietschel ET (1990) Structure-activity relationships in lipopolysaccharides of Bacteroides fragilis. *Rev Infect Dis* 12 Suppl 2:S133-141.
Lu A, Cho K, Black WP, Duan X-y, Lux R, Yang Z, Kaplan HB, Zusman DR,Shi W (2005) Exopolysaccharide biosynthesis genes required for social motility in Myxococcus xanthus. *Molecular Microbiology* 55(1):206-220.
Maclean L, Perry M, Nossova L, Kaplan H,Vinogradov E (2007) The structure of the carbohydrate backbone of the LPS from Myxococcus xanthus strain DK1622. *Carbohydrate research* 342:2474-2480.
Marks KM & Nolan GP (2006) Chemical labeling strategies for cell biology. *Nature Methods* 3(8):591-596.
Metzger LEt & Raetz CR (2010) An alternative route for UDP-diacylglucosamine hydrolysis in bacterial lipid A biosynthesis. *Biochemistry* 49(31):6715-6726.
Mozaheb N & Mingeot-Leclercq M-P (2020) Membrane Vesicle Production as a Bacterial Defense Against Stress. *Frontiers in Microbiology* 11(3120).
Mullineaux CW, Nenninger A, Ray N,Robinson C (2006) Diffusion of green fluorescent protein in three cell environments in Escherichia coli. *J Bacteriol* 188(10):3442-3448.
Nan B & Zusman DR (2011) Uncovering the mystery of gliding motility in the myxobacteria. *Annu Rev Genet* 45:21-39.
Nilsson I, Grove K, Dovala D, Uehara T, Lapointe G,Six DA (2017) Molecular characterization and verification of azido-3,8-dideoxy-d-manno-oct-2-ulosonic acid incorporation into bacterial lipopolysaccharide. *The Journal of biological chemistry* 292(48):19840-19848.
Nilsson I, Prathapam R, Grove K, Lapointe G,Six DA (2018) The sialic acid transporter NanT is necessary and sufficient for uptake of 3-deoxy-d-manno-oct-2-ulosonic acid (Kdo) and its azido analog in Escherichia coli. *Molecular Microbiology* 110(2):204-218.
Nwe K & Brechbiel MW (2009) Growing applications of "click chemistry" for bioconjugation in contemporary biomedical research. *Cancer biotherapy & radiopharmaceuticals* 24(3):289-302.
Okuda S, Sherman DJ, Silhavy TJ, Ruiz N,Kahne D (2016) Lipopolysaccharide transport and assembly at the outer membrane: the PEZ model. *Nature reviews. Microbiology* 14(6):337-345.
Palsdottir H, Remis JP, Schaudinn C, O'Toole E, Lux R, Shi W, McDonald KL, Costerton JW,Auer M (2009) Three-dimensional macromolecular organization of cryofixed Myxococcus xanthus biofilms as revealed by electron microscopic tomography. *J Bacteriol* 191(7):2077-2082.

Pathak DT, Wei X, Bucuvalas A, Haft DH, Gerloff DL,Wall D (2012) Cell contact-dependent outer membrane exchange in myxobacteria: genetic determinants and mechanism. *PLoS Genet* 8(4):e1002626.

Ravicoularamin G (2019) *SYNTHESIS OF POTENTIAL INHIBITORS AND SIDEROPHORE CONJUGATES OF KDO-PROCESSING ENZYMES*. MASTER OF SCIENCE IN EXPERIMENTAL HEALTH SCIENCES (Institut National de la Reserche Scientifique Institut Armand-Frappier).

Remis JP, Wei D, Gorur A, Zemla M, Haraga J, Allen S, Witkowska HE, Costerton JW, Berleman JE,Auer M (2014) Bacterial social networks: structure and composition of Myxococcus xanthus outer membrane vesicle chains. *Environ Microbiol* 16(2):598-610.

Selvaraj R & Fox JM (2013) trans-Cyclooctene--a stable, voracious dienophile for bioorthogonal labeling. *Current opinion in chemical biology* 17(5):753-760.

Sharpless KB (2002) A stepwise huisgen cycloaddition process: copper(I)-catalyzed regioselective "ligation" of azides and terminal alkynes. *Angewandte Chemie (International ed. in English)* 41(14):2596-2599.

Silhavy TJ, Kahne D,Walker S (2010) The bacterial cell envelope. *Cold Spring Harbor perspectives in biology* 2(5):a000414-a000414.

Smukalla S, Caldara M, Pochet N, Beauvais A, Guadagnini S, Yan C, Vinces MD, Jansen A, Prevost MC, Latgé JP, Fink GR, Foster KR,Verstrepen KJ (2008) FLO1 is a variable green beard gene that drives biofilm-like cooperation in budding yeast. *Cell* 135(4):726-737.

Takayama Y, Kusamori K,Nishikawa M (2019) Click Chemistry as a Tool for Cell Engineering and Drug Delivery. *Molecules* 24(1).

ThermoFisher (2020) Vibrant DiO Cell-Labeling Solution.

Thorn K (2017) Genetically encoded fluorescent tags. *Molecular biology of the cell* 28(7):848-857.

van den Berg B (2010) Going forward laterally: transmembrane passage of hydrophobic molecules through protein channel walls. *Chembiochem* 11(10):1339-1343.

Velicer GJ & Yu YT (2003) Evolution of novel cooperative swarming in the bacterium Myxococcus xanthus. *Nature* 425(6953):75-78.

Vollmer W, Blanot D,De Pedro MA (2008) Peptidoglycan structure and architecture. *FEMS Microbiology Reviews* 32(2):149-167.

Vorachek-Warren MK, Ramirez S, Cotter RJ,Raetz CR (2002) A triple mutant of Escherichia coli lacking secondary acyl chains on lipid A. *The Journal of biological chemistry* 277(16):14194-14205.

Vuorio R & Vaara M (1995) Comparison of the phenotypes of the lpxA and lpxD mutants of Escherichia coli. *FEMS Microbiol Lett* 134(2-3):227-232.

Wang J, Hu W, Lux R, He X, Li Y,Shi W (2011) Natural transformation of Myxococcus xanthus. *Journal of bacteriology* 193(9):2122-2132.

Wei X, Vassallo CN, Pathak DT,Wall D (2014a) Myxobacteria produce outer membrane-enclosed tubes in unstructured environments. *J Bacteriol* 196(10):1807-1814.

Wei X, Vassallo CN, Pathak DT,Wall D (2014b) Myxobacteria produce outer membrane-enclosed tubes in unstructured environments. *Journal of bacteriology* 196(10):1807-1814.

Weski J & Ehrmann M (2012) Genetic analysis of 15 protein folding factors and proteases of the Escherichia coli cell envelope. *Journal of bacteriology* 194(12):3225-3233.

Whitfield Ra (2002) Lipopolysaccharide endotoxins. *Annu Rev Biochem* 71:635-700.

Zusman DR, Scott AE, Yang Z,Kirby JR (2007) Chemosensory pathways, motility and development in Myxococcus xanthus. *Nature Reviews Microbiology* 5(11):862-872.